# **Energy consumption model of Binder-Jetting Additive Manufacturing Processes**

Xin Xu

Mechanical Engineering

McGill University, Montreal

August 2014

A thesis submitted to McGill University in partial fulfillment of the requirements of the degree of MEng (Thesis)

© Xin Xu 2014

**Energy consumption model of Binder-Jetting Additive** 

**Manufacturing Processes** 

By

Xin Xu

Abstract:

Considering the potential for new product design possibilities and the reduction of

environmental impacts, Additive Manufacturing (AM) technologies are considered to

possess significant advantages for automotive, aerospace and medical equipment

industries. However, there is very limited research about energy and material

consumption aspects of AM, which prevents evaluating the sustainability of AM. This

paper presents a simulation method to calculate the energy and material consumption

for AM. Based on this method, an energy and material consumption model of Binder-

Jetting technology is created. Binder-Jetting (BJ) is one of the commercial AM

technology which can process a variety of materials including stainless steel, ceramic,

polymer and glass. Decomposition is performed to analyze the BJ printing process. A

power analyzing method is developed to provide the power information for BJ model.

Based on the analyses, total energy and material consumption is calculated as a function

of part geometry and printing variables. Finally, test validation is performed to check

the validity of the BJ model and simulation method. Case studies are performed to

reveal the energy and material consumption characteristics of BJ process. This process

model provides a tool to optimize part geometry design and print variables choosing

with respect to energy and material consumption.

Thesis supervisor: Prof. Fiona Zhao

Résumé

En considerant du potentiel de nouvelles possibilités de conception de produits et la

réduction des impacts environnementaux, Additive Manufacturing(AM) technologies

sont considérés comme possédant des avantages importants pour l'automobile, de

l'a <del>c</del>rospatiale et de l'<del>c</del>quipement m <del>c</del>dical industries. Cependant, il ya très peu de

recherche sur l'énergie et la consommation de mati ère aspects de AM, ce qui emp êche

l'évaluation de la durabilit é des AM. Cet article présente une méhode de simulation

pour calculer les consommations énergétiques et matérielles pour AM. Selon cette

m éthode, un mod de de consommation d'énergie et de mat ériel de technologie Binder-

jets est créé Binder-Jetting (BJ) est l'une des technologies AM commerciale qui peut

traiter une vari ét é de mat ériaux, y compris l'acier inoxydable, c éramique, polymère et

verre. La décomposition est réalis ée pour analyser le processus d'impression BJ. Une

méhode d'analyse de puissance est con qu pour fournir des informations de puissance

pour le mod de BJ. D'apr ès les analyses, les consommations énergétiques et des

mat ériaux totaux sont calcul és en fonction de la g éom érie des pi èces et de variables

d'impression. Enfin, la validation de test est effectu épour v érifier la validit édu mod de

BJ et la méthode de simulation. Sutdies de cas sont réalisées à révêler les

caract éristiques de consommation d'énergie et de matière de processus BJ. Ce mod èle

de processus est un outil pour optimiser la conception de la g éom érie de la pi èce et les

variables d'impression en choisissant à l'égard de l'énergie et des consommations

mat érielles.

Directeur de Thèse: Prof. Fiona Zhao

# Ackonwledgements

I would like to take this opportunity to thanks Prof. Fiona Zhao, my supervisor, for her support and guideline for my graduate study. I would also like to acknowledge the generous support for this research by the Additive Design and Manufacturing Lab (ADML) of McGill University.

I would also like to thanks Prof. Xingyu Liu for graciously agreeing to serve as reviewer of my thesis.

Also, I would like to thank Dr. Yunlong Tang who gives me a lot of advises and suggestion for this research. Thanks for the various discussions we had during the development of this thesis.

A special "thank you" goes out to my friends Pengbo, Elizabeth, Gautam, Simon, Han, Yuhaowei and Michel. They were the ones who made my life in McGill better and cheered me up while I facing difficulties.

# **CONTENT**

CHAPTER 1: MOTIVATION OF RESEARCH	12
1.1 OBJECTIVE AND SIGNIFICANT OF RESEARCH	14
1.2 Scope of Research	15
1.3 OUTLINE OF THESIS	16
CHAPTER 2: LITERATURE REVIEW	18
2.1 LCA AND LCI	18
2.1.1 Methodology and Outline of LCA	19
2.1.2 Process Flow Diagram of LCI Compilation	20
2.1.3 Matrix representation of product system	22
2.2.1 Syntax of IDEF0 model	25
2.2.2 IDEF0 decomposition	25
2.3 STRUCTURE OF STL FILE	26
2.3.1 ASCII STL	27
2.3.2 Binary STL	28
2.4 Power Analyzing Method	29
CHAPTER 3: METHOD OF CALCULATING ENERGY AND	D MATERIAL
CONSUMPTION	32
3.1 Principle of Energy and Material Calculation	33
3.2 Basic Operations and Operation List	34
3.3 Encode Operation List	36

3.4 METHOD OF PART SLICING	
3.4.1 STL File Reader40	
3.4.2 Identify Intersecting Triangle40	
3.4.3 Calculate Intersection on Slicing Plane	
CHAPTER 4: MODELLING OF BJ MANUFACTURING PROCESS44	
4.1 IDEF0 Analysis of BJ Process	
4.2 BASIC OPERATIONS OF BJ PROCESS	
4.2.1 Drying of Printed Layer	
4.2.2 Spreading of New Layer	
4.2.3 Printing of New Layer	
4.3 OPERATION TIME OF BASIC OPERATIONS	
4.3.1 Drying of Printed Layer	
4.3.2 Spreading of New Layer	
4.3.3 Printing of New Layer50	
4.4 MATERIAL CONSUMPTION OF BASIC OPERATIONS	
4.4.1 Consumption of Binder51	
4.4.2 Printing Saturation	
4.4.3 Consumption of Cleaner54	
4.4.4 Consumption of Powder55	
4.5 Method of Power Data Analyzing57	
4.5.1 Data analysis method of learning element:58	
4.5.2 Locate Basic operations59	

4.5.3 Validation of Located Operations	63
4.5.4 Statistical Computation of Valid data	64
4.5.5 Saving Data in Knowledge Base	66
4.5.6 Test sample for Collecting Power Data	67
CHAPTER 5: VALIDATION AND SIMULATION OF TEST CASE	68
5.1 VALIDATION OF BJ MODEL	68
5.1.1 Interface of Simulation Program	70
5.1.2 Simulation of different part geometries	71
5.1.3 Simulation of different Process Variable	74
5.2 SIMULATION OF TEST CASES	77
5.2.1 Effects of Layer Thickness	77
5.2.2 Effects of Internal Lattice Structure	79
5.2.3 Sensitivity of Print Orientation	81
CHAPTER 6: CONCLUSION AND FUTURE SCOPE OF RESEARCH.	87
6.1 Conclusions	87
6.2 FUTURE SCOPE OF RESEARCH	89

# LIST OF FIGURES

FIG. 1: BOUNDARY OF BJ MODEL
Fig. 2: Framework of LCA (ISO 14040: 2006)
FIG. 3: PROCESS FLOW OF A TOASTER
FIG. 4: SYNTAX OF IDEFO. "ARROW POSITIONS AND ROLES." PAGE 11, DRAFT
FEDERAL INFORMATION PROCESSING STANDARDS PUBLICATION 183, 1993
DECEMBER 21, ANNOUNCING THE STANDARD FOR INTEGRATION DEFINITION
FOR FUNCTIONMODELING (IDEF0)25
Fig. 5: Decomposition Structure of IDEF0. "Decomposition Structure."
PAGE 15-16, DRAFT FEDERAL INFORMATION PROCESSING STANDARDS PUBLICATION
183, 1993 DECEMBER 21, ANNOUNCING THE STANDARD FOR INTEGRATION
DEFINITION FOR FUNCTIONMODELING (IDEF0)26
FIG. 6: TRIANGULAR FACET OF STL FILE
Fig. 7: Workflow of Energy and Material Simulation
Fig. 8: Structure of Operation List
Fig. 9: Relation between the Properties of Operation Cell
Fig. 10: Workflow of Operation List Encoding
FIG. 11: WORKFLOW OF PART SLICING
FIG. 12: STRUCTURE OF TRIANGLE LIST AND VERTEX LIST40
FIG. 13: STRUCTURE OF TOP AND BOTTOM LIST41
Fig. 14: Possible Position Relations between Triangles and Slicing Plane
$\Delta 1$

FIG. 15: COMPUTATION OF INTERSECTION POINT	43
Fig. 16: Activity A-0	44
Fig. 17: Activity A0	45
Fig. 18: Activity A2	45
FIG. 19: DRYING SYSTEM OF BJ PRINTER	46
Fig. 20: Spreading system of BJ printer	47
Fig. 21: Schematic of Print Bed	49
Fig. 22: Motion of Spreading	49
Fig. 23: Contour of Slice	51
Fig. 24: Scheme of Powder Packing	52
Fig. 25: Workflow of Power Analyzing System	57
Fig. 26: Structure of Power Data	58
Fig. 27: Detecting Edges on Power Curve	59
Fig. 28: Power Curve and Its' First Derivative	60
Fig. 29: Filtered FDP curve	61
Fig. 30: Peaks on The Filtered FDP Curve	62
Fig. 31: Located basic operations	63
Fig. 32: Example of Valid Operation Interval and Inva	ALID OPERATION
Interval	64
Fig. 33: Clustering of Operations	65
Fig. 34: Structure of Data in Knowledge Base	66
Fig. 35: Test Sample for Collecting Power Data	67

Fig. 36: User Interface of Simulation Program70
Fig. 37: Geometries for Printing Test
Fig. 38: Power Curves of Simulation Results and Experimental Records73
Fig. 39: Geometry of Compression Test Cylinders
Fig. 40: Geometry of Compressor Wheel
Fig. 41: Internal Lattice Structure of Different Strut Thickness80
FIG. 42: LH AND SH ON A PART82
FIG. 43: GEOMETRY OF MECHANICAL SUPPORT AND SPRING
Fig. 44: Energy Consumption of Different Print Orientation
FIG. 45: LH AND SH OF CUBOID85
FIG. 46: LSR vs. RMM for Cuboid86

# Chapter 1: Motivation of Research

Additive Manufacturing (AM) (also known as Layered Manufacturing (LM)/Solid Freeform Fabrication (SFF)) refers to a group of manufacturing technologies which evolved from the Rapid Prototyping (RP) technique. For both AM and RP process, the basic principle of creating part is the same: fabricating parts by generating contiguous slices layer by layer. AM technologies can be differentiate by how the slices being generated. Several different slice generating techniques have been developed over years. Some of the most popular AM technologies which have already been commercialized are classified here by the slicing generating techniques:

**Binder-Jetting (BJ)**: Using liquid binder to glue powders (metal or glass powders) together and from the designed part shape. Then the part is sintered by a sintering furnace.

**Stereolithography** (**SLA**): Using ultraviolet laser to cure actinic photopolymer liquid and form the designed shape.

Laser Sintering (SLS), Direct Metal Laser Sintering (DMLS) and Selective Laser Melting (SLM): Using laser power to sinter or melt powders (metal, polymer or ceramic powder).

**Electron Beam Melting (EBM)**: Using high power electron beam to melt metal powder.

**Fused Deposition Modeling (FDM)**: Extruding or depositing molten material to form the design part.

The difference between AM and RP is the application of their product. The RP aims to create prototype products for conceptualization or visualization exhibition while the AM technologies are used to manufacture functional parts in industry. Compared with traditional manufacturing technologies, AM technologies provide more design freedom for innovative product and AM remove the traditional manufacturing restrictions (enable fabricate complex inner shapes for example) [1].

Moreover, the potential environmental benefit is also one of the strong mainstays of development for the AM technologies for the next 10 year [2]. Nowadays,

sustainability takes an increasingly important place in the industrial world. The reason for this is because the manufacturing is consuming a huge amount of energy and generating grate burden to the environment. According to a report of [3], manufacturing is response for 90% of energy consumption and 84% of energy-related CO2 emission in the industry sector. Furthermore, in the scenario of an energy research which conducted by the International Energy Agency (IEA), this industrial energy consumption will keep the fastest growing one when compared to other sectors (transportation, residential and commercial) until 2050 [4]. Therefore, it appears critical to find out ways to reduce the energy and material consumption in the manufacturing process. AM technologies, from general view, are seen as "cleaner" processes compare to the traditional manufacturing technologies. As aforementioned, in AM, parts are fabricated by creating continuous slices on top of each other. As a result, materials are only used to form products, which means AM technologies can consume the exact amount of material while conventional machining produces waste material. In addition, the only tool of AM is the AM machine contrary to conventional machining which using a series of machining tools (for instance such as stamping, turning, milling and drilling) [5]. Hence, AM can reduce the life cycle material mass and energy consumption by eliminating scrap and ancillary process. Another advantage of AM process is, resulting to its' high concentricity, this characteristic affords possibility of reducing the transportation energy consumption [6]. Possessing these good environmental characteristics, AM technologies have great potential to make the manufacturing more sustainable.

Insofar, as our society concerns more and more on the environmental problems, as well as legislation about environment has become prominent (Normalization ISO 14 044), the environmental impacts of the AM technologies have been evaluated to make them be easier accepted by the industrial world. Some research has been conducted on the energy consumption of machine tools of the AM (standby consumption, in process consumption, leaser energy consumption of SLS, etc.). But only a few studies take into account the materials flows. As a result, the Life-Cycle Inventory (LCI) data of AM technologies are often incomplete. Because of the lack of well documented Life-Cycle

Inventory data, it is difficult to conduct an exact Life-Cycle Assessment (LCA), which restrict providing a comprehensive analysis on the sustainability aspect of AM technologies.

These insufficiencies of energy and material consumption of AM technologies provide the motivation to carry out this research. And to take a step forward, this study aims to provide a method to calculate energy and material consumption of AM technologies.

# 1.1 Objective and Significant of Research

The energy and material consumption of conventional machining tool has been researched and modelled for years. Different methods are developed to simulate and optimize the energy or material consumption of the machining process (such as turning, milling and drilling) [7-10]. However, the manufacturing processes of AM technologies are quite different from the conventional manufacturing processes which fabricate parts by removing the un-desired material to achieve the desired shapes. On the contrary, AM create parts by generating contiguous slices. Thus, the process of AM can be seen as process to accumulate the materials of part together and form the desired shapes, which is how the name of AM originated. Since the fabrication processes of AM are totally on the opposite side of conventional manufacturing processes, the process parameters, models and simulation method which developed for the conventional manufacturing processes are no longer suitable for the AM process. Hence, an effective simulation method is needed to model the energy and material consumption of AM technologies.

This research dedicates to develop such an effective simulation method to calculate the energy and material consumption of AM technologies. The method developed by this research will contribute to the landscape of AM technologies in the following aspects:

Developing a new energy and material simulation method for AM technologies.
 The simulation results then provide information to build the LCI for AM technologies. Furthermore, LCI data can support the LCA or cost analyses. Based

- on these analyzing works, manufacturer can tell if a product is suitable to AM and which kind of AM technology should be used to fabricate the product.
- 2. By this method, AM engineers or practitioners are able to predict the energy and materials been consumed to fabricate an AM part before the part is really fabricated. Thus, this method can be used as a tool to evaluate the energy and material costs for a specific design. Based on this tool, optimization algorithms can be developed to achieve the optimal part geometry or process parameters and improve the environmental performance of the design.

#### 1.2 Scope of Research

The energy and material analysis can be conducted on different levels depending on the scope of research. Before conducting the research, the scope and the boundaries of the research should be defined first. According to the research of Duflou et al [11], five different levels can be identified: device/process level, line/cell/multi-machine system, facility, multi-factory system and enterprise/global supply chain. Each one of above analysis levels relies on different assumptions, different input and provides different results. In this research, we focus on the unit-process level of AM technologies. Thus we are focusing on the individual manufacturing device or machine of AM technologies, which is defined as unit process. Also, support equipment of the unit process is included here, such as material feed system, control system of the machine and ventilation system. We only consider about the energy and material flows which are directly input to or output from the device or machine. The upstream and downstream costs of the materials and energy, such as the energy used to produce the steel power or the energy and materials used to dispose the waste, are not considered in this model. To give a instance, for the BJ model which developed in Chapter 4, the boundary of the model is shown as

Fig. 1:

The boundary of the BJ model is shown as the red box in

Fig. 1. Hence, the BJ model only considers the printing process. The inputs of the model are the STL (STereo-Lithography) file, print orientation and process variables

(represented as green arrows). Based on this information, the model will calculate the usage of electricity, power, binder and cleaner (represented by blue arrows).

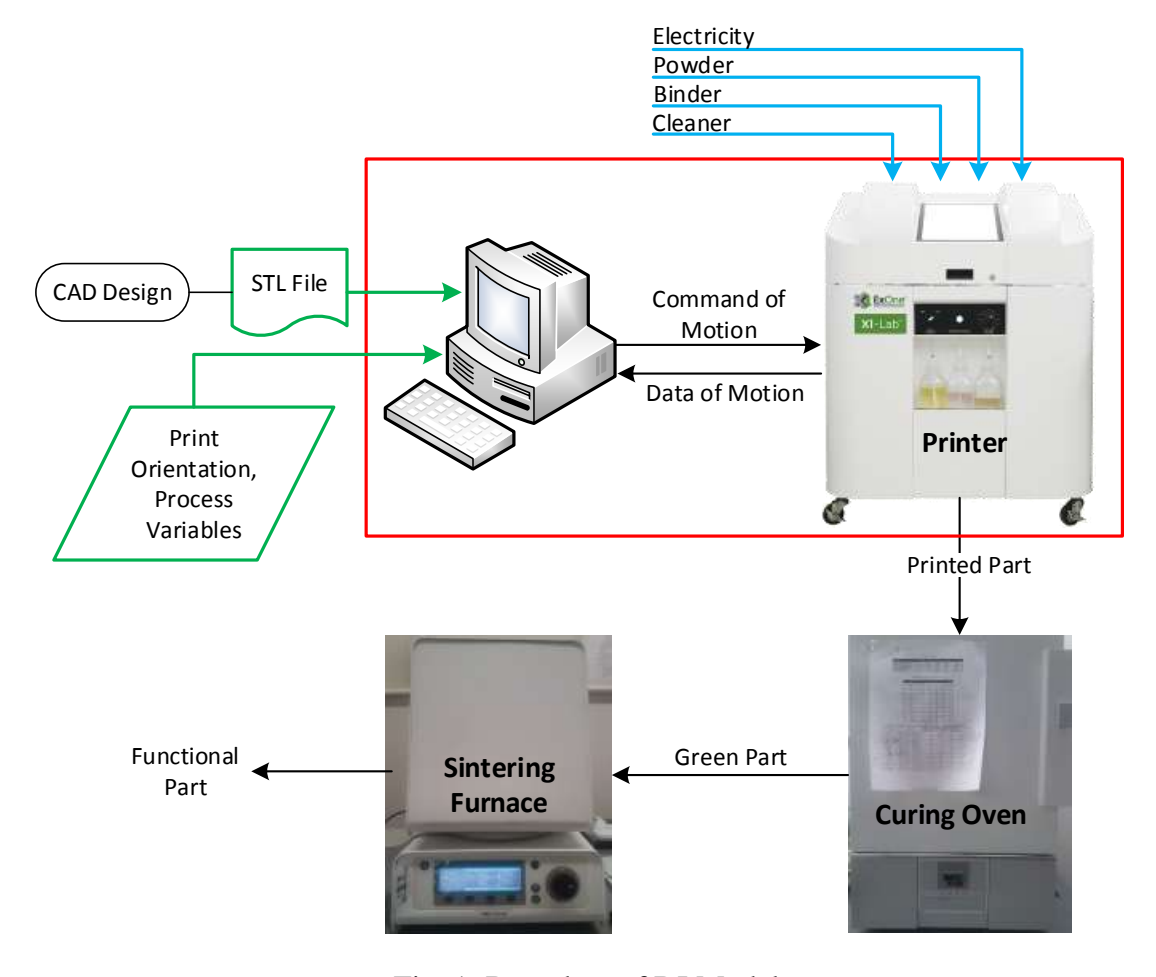


Fig. 1: Boundary of BJ Model

The curing oven and sintering furnace also contribute to the part manufacturing. However, these two operations are well developed traditional manufacturing processes which are not only developed for AM technologies. And there are already a lot of research and models for these two processes. The curing and sintering are not considered in the unit process model

#### 1.3 Outline of Thesis

The rest of the thesis is divided into five chapters. Chapter 2 reviews the relevant published literatures in the area of sustainability of manufacturing, energy and material consumption of AM, and the mathematical tools of power analyzing. Then, Chapter 3 proposed the energy and material simulation method for AM technologies. In Chapter 4, the method is adapted to the BJ technology. The printing process of BJ is analyzed

to obtain the process time, power and material consumption information. By filling this information into the simulation method, an energy and material consumption model of BJ is created. Afterward, Chapter 5 performs validation of the BJ model and provides several material and energy consumption calculation of test cases of BJ technology. Finally, in Chapter 6, the conclusions of this research are summarized and the scope of future research is presented.

# Chapter 2: Literature Review

This research dedicates to develop a simulation method to calculate the energy and material consumption of AM technologies. Or from the perspective of LCA, this research aims to provide the LCI data for AM technologies. Therefore, published literatures which relevant to LCI and energy or material consumption models of manufacturing are reviewed here to provide a thorough understanding of the research areas of LCA and form a fundamental of this research. In addition, as the simulation method will be adapted to BJ technology, materials about IDEF0 method is review here and the IDEF0 method will be applied in Chapter 4. As the STL file is used to import the part geometry into the simulation method, introduction of this file format will be presented. Moreover, as the energy data of the printing process of BJ will be processed to provide the energy information for simulation, literatures relevant to energy analyzing approach are also included in this chapter. The following sections present these literatures by their subject areas.

#### 2.1 LCA and LCI

"Life Cycle Assessment (LCA) is a structured, comprehensive and internationally standardized method. It quantifies all relevant emissions and resources consumed and the related environmental and health impacts and resource depletion issues that are associated with any goods, services or products." [12]. As the LCA will consider all of energy consumption, resources consumption and environmental and health impact associated with products, it has to take into account of the full life-cycle of a product. Thus, from the extraction of resources, through production, usage and up to the Endto-Life stage. According to Ashby [13] the whole life cycle of a product can be divided into five phases: the raw materials extraction, the manufacturing, the transportation, the use phase and the disposal. Due to this characteristic, LCA can avoid resolving one environmental problem while creating others; for example, increasing upstream energy consumption while improving production technology. As a result, LCA is considered as a reliable and powerful tool to help make decisions, complementing other methods and provide data for sustainability analysis.

## 2.1.1 Methodology and Outline of LCA

LCA is a phased and systematic approach [12]. According to Ashby [13], it consists of four components as shown in :

- Goal definition and scoping: Define and describe the product, process and activity.
   Establish the context in which the assessment is to be made as well as identify boundaries and environmental impacts to be reviewed for the assessment.
- 2. Inventory analysis: Identify and quantify energy, resources and material usage and environmental release.
- Impact assessment: Assess the potential human and ecological effects of energy, resources and material usage and environmental release identified in the inventory analysis.
- 4. Interpretation: Evaluate the results of inventory analysis and impact assessment to select the preferred product, process or service with a clear understanding of uncertainty and the assumption used to generate the result.

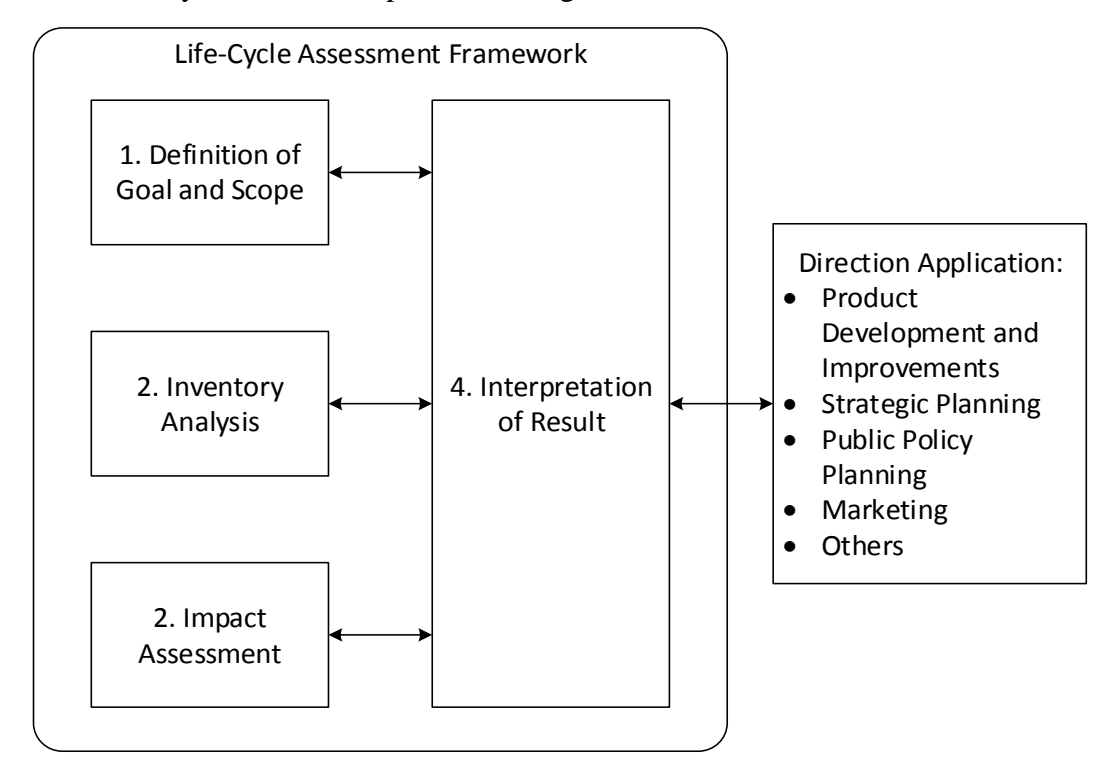


Fig. 2: Framework of LCA (ISO 14040: 2006)

In the second step of LCA, the inventory analysis is also called the LCI of LCA. In ISO 14040 [14], LCI is defined as a phase of LCA which compile and quantify inputs

and outputs of a given product system throughout its life cycle. LCI data then are the result of this phase. To some extent, LCI data are a list which containing the quantities of energy and materials consumed and pollutants released. Therefore, from this point, the simulation method can be seen as a tool to provide the LCI data for LCA. Hence, understanding how the LCI data been calculated and complied will contribute to develop the simulation method. As a result, the materials of LCI compilation are reviewed in the section 2.1.2 and 2.1.3.

#### 2.1.2 Process Flow Diagram of LCI Compilation

Process flow diagram method is the most straight forward way to calculate LCI data. As the name suggests, this compilation is based on a process flow diagram. It appears in early LCA researches and guidelines such as works of [15], [16] and [17] Result from this, it become compilation method of LCI research. A brief sample of this method is given in research of [18]. As shown in Fig. 3, a process flow diagram shows how the commodity flows connect the processes together of a toaster product system.

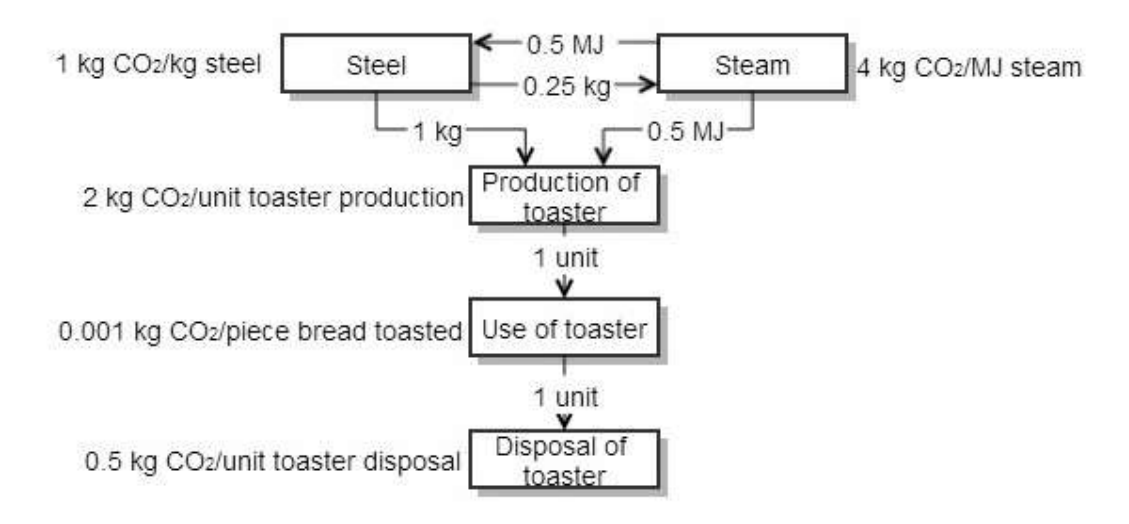


Fig. 3: Process Flow of a toaster

In Fig. 3, boxes represent processes and arrows represent commodity flows. For each process, there is a ratio of between a number of inputs and outputs. In this example, assumptions are made as following:

A toaster is produced from 1 kg of steel and 0.5 MJ of steam while generate 2 kg of CO2. Producing 1 kg of steel requires 0.5 MJ of steam and generates 1 kg of CO2.

Producing 1 MJ of steam needs 0.5kg of steel and generates 4 kg of CO2. The life-time of a toaster is toast 1000 times. Toasting 1 piece of bread generate 0.001 kg of CO2 and disposal of toaster generate 0.5 kg of CO2.

This above provides the fundamental data for LCI calculation. After collecting data, plain algebra is performed to calculate the amount of energy, material consumed and emission generated to obtain a certain functional unit. For the product system of the toaster, let's define the functional unit as 'production of 1000 pieces of bread'. Then the LCI calculation is conducted out as following:

The emission of CO2: 
$$\left(\frac{1 \, kg \, CO_2}{kg \, steel} \cdot 1 \, kg \, steel\right) + \left(\frac{4 \, kg \, CO_2}{MJ \, steam}\right)$$

$$0.5 \, MJ \, steam\right) + \left(\frac{2 \, kg \, CO_2}{unit \, toaster \, prod.} \cdot 1 \, unit \, toaster \, prod.\right) + \left(\frac{0.001 \, kg \, CO_2}{piece \, bread \, toasted} \cdot 1000 \, pieces \, bread \, toasted\right) + \left(\frac{0.5 \, kg \, CO_2}{unit \, toaster \, disp.}\right)$$

$$1 \, unit \, toaster \, disp.\right) = 6.5 \, kg \, CO_2$$

However, for the toaster system in the example, another issue needs to be addressed before LCI calculation. In Fig. 3, there is a loop existing between steel and steam which means the steel production process indirectly uses its own output, the steel through steam production. It's also the same situation for the steam. To calculate the emission generated by this kind of loop, [17] proposed a iterative method to find out the answer. For the toaster example, it solved as following:

$$\left(\frac{4 \, kg \, Co_2}{MJ \, steam} \cdot 0.5 \, kg \, steel\right) + \left(\frac{1 \, kg \, Co_2}{kg \, steel} \cdot 0.25 \, kg \, steel\right) + \left(\frac{4 \, kg \, Co_2}{MJ \, steam} \cdot 0.125 \, kg \, steel\right) + \left(\frac{1 \, kg \, Co_2}{kg \, steel} \cdot 0.0625 \, kg \, steel\right) + \left(\frac{4 \, kg \, Co_2}{MJ \, steam} \cdot 0.03125 \, kg \, steel\right) + \cdots$$

$$= \left(\frac{1 \, kg \, Co_2}{kg \, steel} \cdot 0.25 \, kg \, steel\right) + \left(\frac{4 \, kg \, Co_2}{MJ \, steam} \cdot 0.125 \, kg \, steel\right) + \left(\frac{1 \, kg \, Co_2}{kg \, steel} \cdot 0.0625 \, kg \, steel\right) + \left(\frac{4 \, kg \, Co_2}{MJ \, steam} \cdot 0.03125 \, kg \, steel\right) + \cdots$$

Above is a combine of four infinite geometric progressions, they are:

$$(4 \cdot 0.5) \cdot \sum_{0}^{n} 0.25^{n} + (1 \cdot 0.25) \cdot \sum_{0}^{n} 0.25^{n} + (1 \cdot 0.25) \cdot$$
 Eq. 3

$$\sum_{0}^{n} 0.25^{n} + (4 \cdot 0.125) \cdot \sum_{0}^{n} 0.25^{n}$$

Since  $\sum_{0}^{n} a^{n} = \frac{1}{1-a}$ , for 0<a<1, Equation 3 is expressed as

$$= 4 \cdot 0.5 \frac{1}{1 - 0.25} + 1 \cdot 0.25 \frac{1}{1 - 0.25} + 1 \cdot 0.25 \frac{1}{1 - 0.25} + 4 \cdot 0.125 \frac{1}{1 - 0.25} = 4$$
Eq. 4

Thus, the total CO2 emission for the toaster system is 6.5 + 4 = 10 kg CO2.

## 2.1.3 Matrix Representation of Product System

Other than process flow diagram method, there are more computational methods to compile and calculate LCI data for a product system. Matrix inversion method is another way to fulfill this LCI calculation work. It was first introduced by Heijungs [19]. In general, Heijungs [19] proposed a system of linear equations to solve the LCI problem. An n by n matrix  $\tilde{\mathbf{A}} = |a_{ij}|$  is defined here as a LCA technology matrix. The element  $a_{ij}$  represents input or output of commodity i which generated by process j in a certain duration. The input and output are noted by positive and negative respectively. Define column vector  $\tilde{\mathbf{x}}$  which  $x_j$  represents the operation time for process j to produce the require output of the system. Thereof, the outputs of the system  $\tilde{\mathbf{y}}$  is given as:

$$\tilde{\mathbf{y}} = \tilde{\mathbf{A}}\tilde{\mathbf{x}}$$
. Eq. 5

This equation can be explained as the amount of a commodity output of a system equals to the amount of produced minus the amount consumed within the system. This is the basic principle for all of LCI calculation. Multiplied both side of Eq.5 by  $\widetilde{A}^{-1}$ , then the total operation time  $\widetilde{x}$  which need to produce commodities  $\widetilde{y}$  is calculated as:

$$\tilde{\mathbf{x}} = \tilde{\mathbf{A}}^{-1}\tilde{\mathbf{y}}$$
 Eq. 6

However, to this stage, the real LCI data is still not calculated out yet. To achieve this goal, a p by n matrix  $\widetilde{\mathbf{B}} = |b_{ij}|$  is defined, where  $b_{ij}$  is the amount of emission or resources i been emitted or consumed by process j during the operation time of  $a_{,j}$ .

While  $\widetilde{A}^{-1}$  is not singular, then the total resources consumption and emission by a system to generate or deliver a certain amount of commodity output are calculated by:

$$\widetilde{\mathbf{M}} = \widetilde{\mathbf{B}}\widetilde{\mathbf{A}}^{-1}\widetilde{\mathbf{k}}.$$
 Eq. 7

In the equation above,  $\widetilde{\mathbf{M}}$  is a matrix of the total resources consumption and emission. In other words, it is the total environment intervention matrix. And  $\widetilde{\mathbf{k}}$  is an arbitrary functional unit vector which is defined by the LCI calculator.

Again, use the toaster example to illustrate this method. The commodity flow of the toaster system is expressed as following LCA technology matrix:

$$\widetilde{\mathbf{A}} = \begin{bmatrix} 1 & -0.5 & -1 & 0 & 0 \\ -0.5 & 1 & -0.5 & 0 & 0 \\ 0 & 0 & 1 & -1 & 0 \\ 0 & 0 & 0 & 1000 & 0 \\ 0 & 0 & 0 & 1 & -1 \end{bmatrix}.$$
 Eq. 8

In the above matrix, from left to right, columns stand for steel production, steam production, toaster production, toaster usage and disposal respectively. From upside to downside, rows are assigned as steel (kg), steam (MJ), toaster (unit), toasted bread (piece) and disposed toaster (unit). The environment intervention matrix  $\tilde{\mathbf{B}}$  and functional vector  $\tilde{\mathbf{k}}$  are given by:

$$\widetilde{\mathbf{B}} = [1 \ 4 \ 2 \ 1 \ 0.5]$$
 Eq. 9

and

$$\tilde{\mathbf{k}}^T = [0 \quad 0 \quad 0 \quad 1000 \quad 0].$$
 Eq. 10

respectively. The LCI data of the toaster is calculated according to Eq.7 as  $\widetilde{\mathbf{M}} = \widetilde{\mathbf{B}}\widetilde{\mathbf{A}}^{-1}\widetilde{\mathbf{k}} = 10.5\,$  kg CO2, which is consistent with the result calculated by process flow diagram.

As discussed above, no matter what kind of method is used to conduct the LCI (either process flow diagram or matrix inversion method), the energy and material consumption information of each operation of the process is the foundation to calculate LCI. Therefore, before the LCI calculation, one of the first works is always analyzing the whole process, decomposing the process into a series of operations and identifying

the consumables of each operation. In Chapter 3, this principle is also used while developing the simulation method.

## 2.2 IDEF0 method

IDEF0 is the acronym of Icam DEFinition for Function Modeling where Icam is the acronym of Integrate computer aid manufacturing. It is a function modelling methodology to describe manufacturing functions [20]. This methodology is derived from a well-developed graphic language which named as structured analysis and design technique (SADT) [21]. Commissioned by the US Air Force, SADT developers developed the function modelling method IDEF0 for analyzing and communicating the functional perspective of manufacturing system. In the IDEF0 method, three kinds of information of manufacturing organization or system are modelled in graphical form: the decisions, action and activities. It provides an effective method for the user to analyze the manufacturing enterprise. Furthermore, as IDEF0 model can conduct analysis either for particular functional analysis or for future analysis [22], it can be used as a tool to simulate and optimize the manufacturing system. As an analytical tool, IDEF0 help the researchers identify the functions of a manufacturing system and the consumables information which are needed to perform the functions. Thus, IDEF0 models are often created as the first task for the system analyzer. As the IDEF0 method can identify the activities and consumables of a manufacturing process, in this research, IDEF0 method is used to analyze the BJ manufacturing process and identify the subprocess and basic operations for the BJ technology.

For its' practical usage, IDEF0 method has been widely used in research and discussed in literature. Busby and Williams [23], and Bravoco and Yadav [24] provided a comprehensive illustration of how to use the IDEF0 method to develop manufacturing system models and the limitation of this method. Sarkis and Lin [25] discussed about the application of overall enterprise modelling for CIM strategic implementation. Kusiak, Nick Larson and Wang [26] present a detailed description of IDEF0 and IDEF3 approaches and illustrate an algorithm for analyzing IDEF models, which demonstrate

the usage of IDEF models for reengineering of design and manufacturing process. In the research of Kim, Kim and Choi [27], they developed an methodology called OOMIS (Object-Oriented modeling methodology for Manufacturing Information Systems). IDEF0 approach is used to create functional diagrams for the OOMIS methodology.

#### 2.2.1 Syntax of IDEF0 model

The IDEF0 model diagram is based on a simple syntax shown as Fig. 4. For each activity, it is represented by a box with a verb-based label. Inputs for the activity are shown as arrows entering the left side of the box and outputs are shown as arrows leaving from the box on the right side of the box. Controls of the activity are represented as the arrows entering the top of the box while the mechanisms are represented as arrows entering the bottom of the box. Inputs, Controls, Outputs and Mechanisms (ICOMs) are all referred to as concepts.

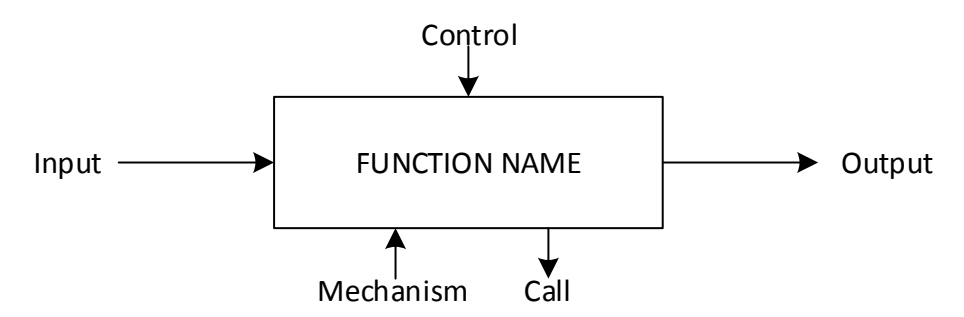


Fig. 4: Syntax of IDEF0. "Arrow Positions and Roles." Page 11, Draft Federal Information Processing Standards Publication 183, 1993 December 21, Announcing the Standard for INTEGRATION DEFINITION FOR FUNCTIONMODELING (IDEF0)

#### 2.2.2 IDEF0 Decomposition.

IDEF0 model is a useful tool to analyze a complex process and decompose it into simple operations. A strategy to create and organize an IDEF0 model is to build a hierarchical decomposition of activities. As shown Fig. 5:

A border of an IDEF0 diagram represents the boundaries drawn around certain activity. Inside the border, an activity is decomposed into smaller activities, which together form the box in a higher level diagram. By building this hierarchical structure,

a multi-level model of a process is created. As these multi-level models progressively reveal the details of activities, the basic operations which made up the process are identified.

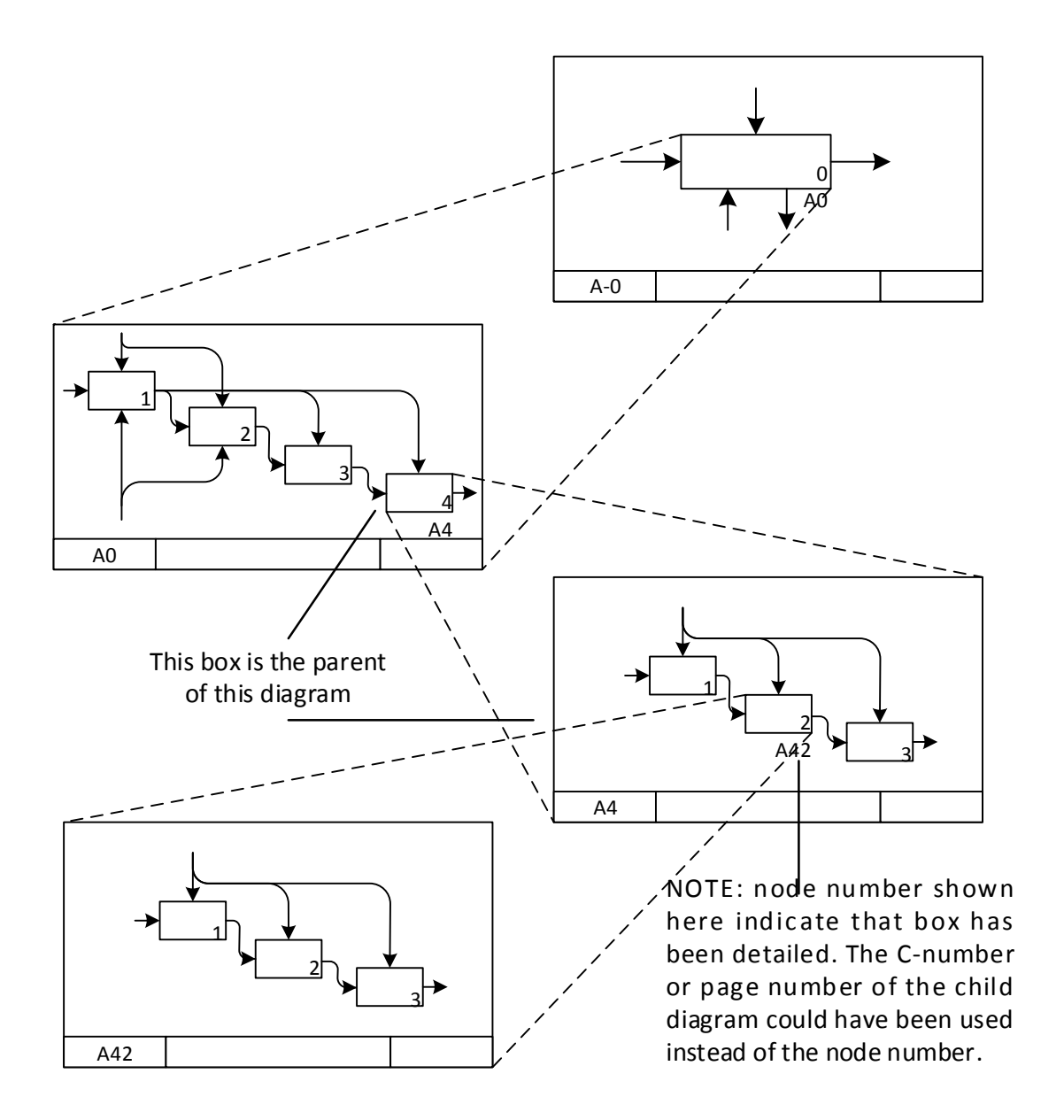


Fig. 5: Decomposition Structure of IDEF0. "Decomposition Structure." Page 15-16,
Draft Federal Information Processing Standards Publication 183, 1993 December 21,
Announcing the Standard for INTEGRATION DEFINITION FOR
FUNCTIONMODELING (IDEF0)

# 2.3 Structure of STL file

In this research, STL is used to import the part geometry into the simulation model. Also, because of its' advantages of sample structure and ease of use, nearly all of the RP and AM process use it as the geometry input format [28]. As AM processes fabricated part by creating slices layer by layer, the geometry of each slice is required. For the same reason, the geometry information of each slice is also needed for the simulation method. A slicing method is developed in Chapter 3 to slice the STL file and achieve this information. In order to conduct the slicing, the structural features of STL file are discussed here:

STL is a file format of a stereolithography CAD software which is created by 3D Systems Company.

As shown in Fig. 6, STL represent the geometry of the part by triangular facet. Hence, the STL file is consists of a list of triangular facet data. These triangle facets are described by a unit normal vector and the three vertices (ordered by the right hand rule) of the facet using a three-dimensional Cartesian coordinate system. One constraint of the coordinates is it must be positive numbers.



Fig. 6: Triangular Facet of STL file

The STL format has two representations: ASCII and binary. Usually, binary files are more common, since they are more compact. The detail of the two representation are illustrated as following (courtesy of [29]):

#### **2.3.1 ASCII STL**

An ASCII STL file begins with the line:

solid name

Where name is an optional string (though if name is omitted there must still be a space after solid). The file continues with any number of triangles, each represented as follows:

```
facet normal ni nj nk

outer loop

vertex v1x v1y v1z

vertex v2x v2y v2z

vertex v3x v3y v3z

endloop

endfacet
```

Where each n or v is a floating point number in sign-mantissa 'e'-sign-exponent format, e.g., "-2.648000e-002" (noting that each "v" must be non-negative). The file end with:

```
endsolid name
```

White space (spaces, tabs, newlines) may be used anywhere in the file except within numbers or words. However, the spaces between 'facet' and 'normal' and between 'outer' and 'loop' are required.

# 2.3.2 Binary STL

Other than the ASCII STL file, a binary STL file format is also existed and even used more wildly due to its' compact characteristic. A binary STL file has an 80 character header. Following the header is a 4 byte unsigned integer indicating the number of triangular facets in the file. Following that is data describing each triangle in turn. The file simply ends after the last triangle.

Each triangle is described by twelve 32-bit-floating point numbers: three for the normal and then three for the X/Y/Z coordinate of each vertex – just as with the ASCII version of STL. After the twelve floats there is a two byte unsigned 'short' integer that is the 'attribute byte count' – in the standard format, generally, this part is zero. The structure of the file is as following:

UINT8[80] – Header

UINT32 – Number of triangles

foreach triangle

REAL32[3] – Normal vector

REAL32[3] - Vertex 1

REAL32[3] - Vertex 2

REAL32[3] - Vertex 3

UINT16 – Attribute byte count

end

### 2.4 Power Analyzing Method

In Chapter 4, an energy and material consumption model for the BJ technology is created. For this model, the energy data of the printing process of BJ manufacturing process were collected and processed to support the analyzing and model creating. The energy data are recorded as a power versus time curve. All of the power information of the printing process is contained in this curve. The target of the power analyzing is to derive the power information of each sub-operations of the total power curve of the printing process. From this point, the most fundamental function of the power analyzing system is to disaggregate the total power data into individual operations and extract information for further calculation. This function can be achieved by two methods: the DDSC and the NIALM. Articles relative to these two methods are reviewed here respectively.

Compared to the NIALM method, the DDSC method is a relatively new power disaggregation method which developed in the past decade. For this method, researchers put more concentration on disaggregating electricity using low-resolution, hourly data. Also the energy disaggregation is treated as a source separation problem and machine learning techniques are applied to solve the problem. Sparse non-negative tensor algorithm is widely used in the research of source separation. In the research of Figueiredo, Ribeiro and de Almeida [30], the electrical signal source separation problem is treated as a single-channel source separation. A multi-way arrays method

and the corresponding non-negative tensor factorization are employed in their research to analyse a household electrical energy consumption which measured by a single power monitor. Schmidt and Olsson [31] applied a sparse non-negative matrix factorization algorithm to separate multiple speech source from a single microphone recording. Shown as the results of the two researches, the sparse non-negative tensor algorithm is an effective tool to conduct source separation work. Kolter, Batra and Ng [32] developed the discriminative disaggregation sparse coding (DDSC) algorithm and a novel discriminative training procedure. The result of their research showed the DDSC algorithm can significantly improve the accuracy of energy disaggregation.

Except the DDSC algorithm, there is another method called NIALM method to perform the load disaggregation. In the early 1980s, George W. Hart Ed Kern and Fred Schweppe of MIT invented this method to analyze power data [33]. This method was originally proposed to analyse the summed voltage and current signal which are corresponding to household electrical activities [34]. It can deduce what appliances are used in the house, when they are used and the individual energy consumption of them. As the NIALM method only needs the total load data which measured by one power monitor instead of attaching individual monitors on each equipment, it is considered a low cost approach of load research. In the past twenty years, NIALM technology has been applied on electric meters and used to survey the specific power usage in different homes.

While processing the power signal, edge detection algorithm is adapted in the NIALM. Canny [35] presentst a computational approach to detect edges on 1-D signal data. In his research, three criteria are proposed to evaluate the performance of edge detector. The first and most important criterion is the low errors rate, which means the edges in that the edges occur in the signal data or image should not be missed and there should be no spurious response. The edge detector errors have significant influence on the system performance. The second criterion is the edges should be accurately located, which means the points found by the edge detector should close to the "centre" of true edges as much as possible. However, in the research of Canny [35], the former two criteria are considered as not "tight" enough and a third criteria is proposed. The third

criterion is to ensure the detector has only one response to a signal edge. In other words, this criterion circumvents the possibility of multiple responses to a single edge which are caused by noise. These three criteria were represented by a series of differential equations. By solving these equations, Canny [35] verified the Gaussian function is an ideal kernel function for the filter to perform the edge detection task.

Marceau and Zmeureanu [36] presents a computer program to disaggregates the total electricity consumption in a house into the major end uses based on the analysis of current which is measured at the main entrance. The result of their research showed the errors in estimating the energy shares of three major appliances (refrigerator, baseboard heater and water-heater) are less than 10% for most evaluation scenarios. In their research, seven signal processing algorithms are proposed to filter the power signal before the applicant load reorganization. Considering the pages, the details about the seven signal processor are not illustrated here. However, among these processors, two of them are specially designed for the baseboard heater and stove respectively. Thus, their research pointed out that while knowing the types of appliances, special signal filter can be applied to improve the performance of load disaggregation.

# Chapter 3: Method of calculating energy and material consumption

As discussed before, the most distinctive characteristic of the AM is the part is built layer by layer. Basing on this point, an energy and material simulation method which focuses on the operations of layer printing is proposed in this research. The workflow of this method is as Fig. 7.

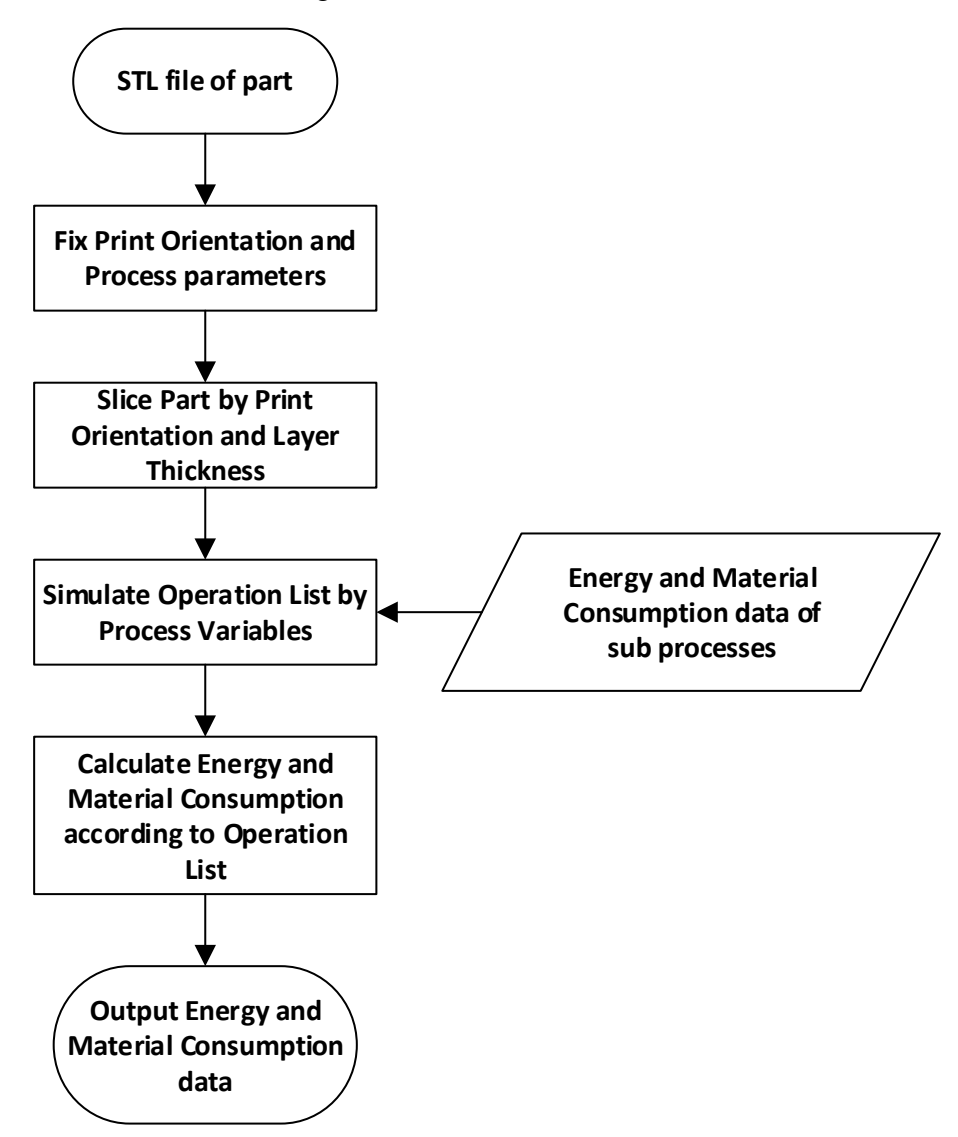


Fig. 7: Workflow of Energy and Material Simulation

As shown in Fig. 7, this method takes account of the influences of part geometry, print orientation and process variable. A part is firstly created by a CAD system and exported as a STL file. Then print orientation and layer thickness are defined to slice part into layers. Based on these layers, an operation list is generated to support the energy and

material calculation. Finally, the results are calculated and output for further research.

The following section will discuss the simulation method in detail.

#### 3.1 Principle of Energy and Material Calculation

Usually, AM technologies are made up of several operations which are influenced by the process variables. Therefore, the energy and material consumption can hardly be directly calculated on the scale of the whole AM process. In order to conduct the modelling and consider about the influence of part geometry and process variables, a method which decompose AM technology into basic operations and simulate the basic operation separately is proposed here. A brief introduction of this method is as following:

Firstly, the whole AM process is divided level by level to obtain the basic operations. After the basic operations being obtained, the manufacturing process is represented by an operation list which is made up of a sequential combination of basic operations. Next, the energy and material consumption of each operation on the operation list is calculated separately according to the part geometry and process variables. Finally, the energy and material consumption is summed to achieve the result for the whole manufacturing process. In summary, the energy consumption of AM technology is calculated as:

$$E = \sum_{i=1}^{n_p} E_i \quad , \tag{Eq. 11}$$

where:

i is the number of operation,

E is the total energy consumption,

 $E_i$  is the energy consumption of operation i,  $i = 1,2,3 ... n_p$ ,

 $n_p$  is the number of sub-processes.

Similarly, the material consumption is calculated as:

$$M_{i} = \sum_{i=1}^{n_{p}} M_{ij}$$
, Eq. 12

where:

 $M_i$  is the total consumption of material j,

 $M_{ij}$  is the consumption of material j by operation i,  $i = 1,2,3...n_p$ .

For the manufacturing process, the power of the AM process is electric power. Therefore the energy consumption then can be calculated as:  $E_i = P_i(t) \cdot dt$ . Substituting the value of  $E_i$ , Eq. 11 can be modified and rewritten as:

$$E = \sum_{i=1}^{n_p} \int_{t_{i,S}}^{t_{i,E}} P_i(t) \cdot dt$$
 . Eq. 13

Where:

 $t_{i,S}$  is the start time of operation i,

 $t_{i.E}$  is the end time of operation i,

 $P_i(t)$  is the electrical power of operation i.

Eq. 12 and Eq. 13 provide two mathematical formulas to calculate the total printing energy material consumption. Using these two equations to do a specific calculation requires to provide following information: the type of operation i, the power of operation i, the material consumption of operation i, the start time of operation i and the end time of operation i. To present the above information, the basic operations and operation list are introduced in the following section.

#### 3.2 Basic Operations and Operation List

As mentioned before, the purpose of introducing the basic operations in this research is to present the manufacturing process by a sequential combination of the basic operations. Therefore, the basic operations are a set of operations which fulfil the following two requirements:

- Combing by a specific sequence, they can represent any printing process of an AM technology.
- These operations are independent to each other. In other words, they cannot be decomposed into other operations in the basic operation set or be made up of other operation in the basic operation set.

# **Operation List**

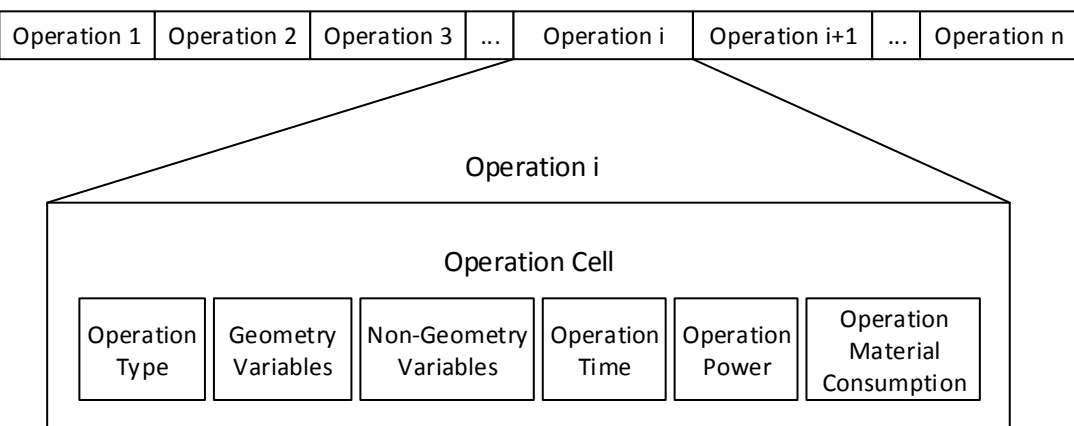


Fig. 8: Structure of Operation List

While the above two requirements are satisfied, the printing process of the AM technology can be represented by a list of basic operations. As shown in the Fig. 8, the operation list is an array of operation cells which arranged in a specific order. The order is determined by the part geometry and process variables. By conducting the basic operations in this order, a designed part is fabricated.

For each operation cell, it is made up of six properties:

- 1. Operation Type: the type of operation. It should be one of the basic operations.
- Geometry Variables: variables which are determined by part geometry and have influences on either of operation time, operation power or operation material consumption.
- Non-Geometry Variables: variables which are not relative to part geometry and have influences on either of operation time, operation power or operation material consumption.
- 4. Operations Time: duration of the operation. It is determined by the operation type, geometry variables and non-geometry variables.
- 5. Operation Power: average power of operation. It is determined by operation type and non-geometry parameters.

6. Operation Material Consumption: the material consumption of operation. It is determined by the operation type, geometry parameters and non-geometry parameters.

The structure of the operation list and operation cell serves for the calculation of energy and material consumption of the printing process. The relation between these properties are shown as Fig. 9.

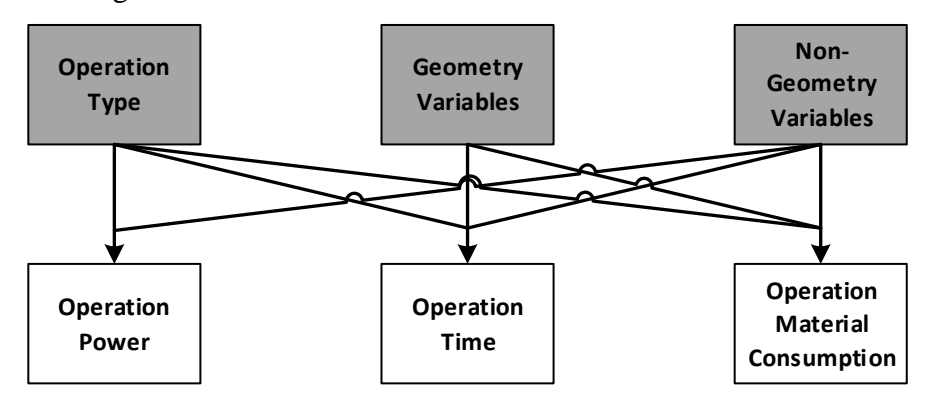


Fig. 9: Relation between the Properties of Operation Cell

For the operation cell, the first three properties contain the necessary information to determine the duration, energy and material consumption of the operation. Therefore, these three properties are defined before the simulation. The last three features are calculated from the former three properties and used for the calculation of the whole process.

#### 3.3 Encode Operation List

An encoding program was developed in this research to create the operation list.

The workflow of this program is shown as the following figure:

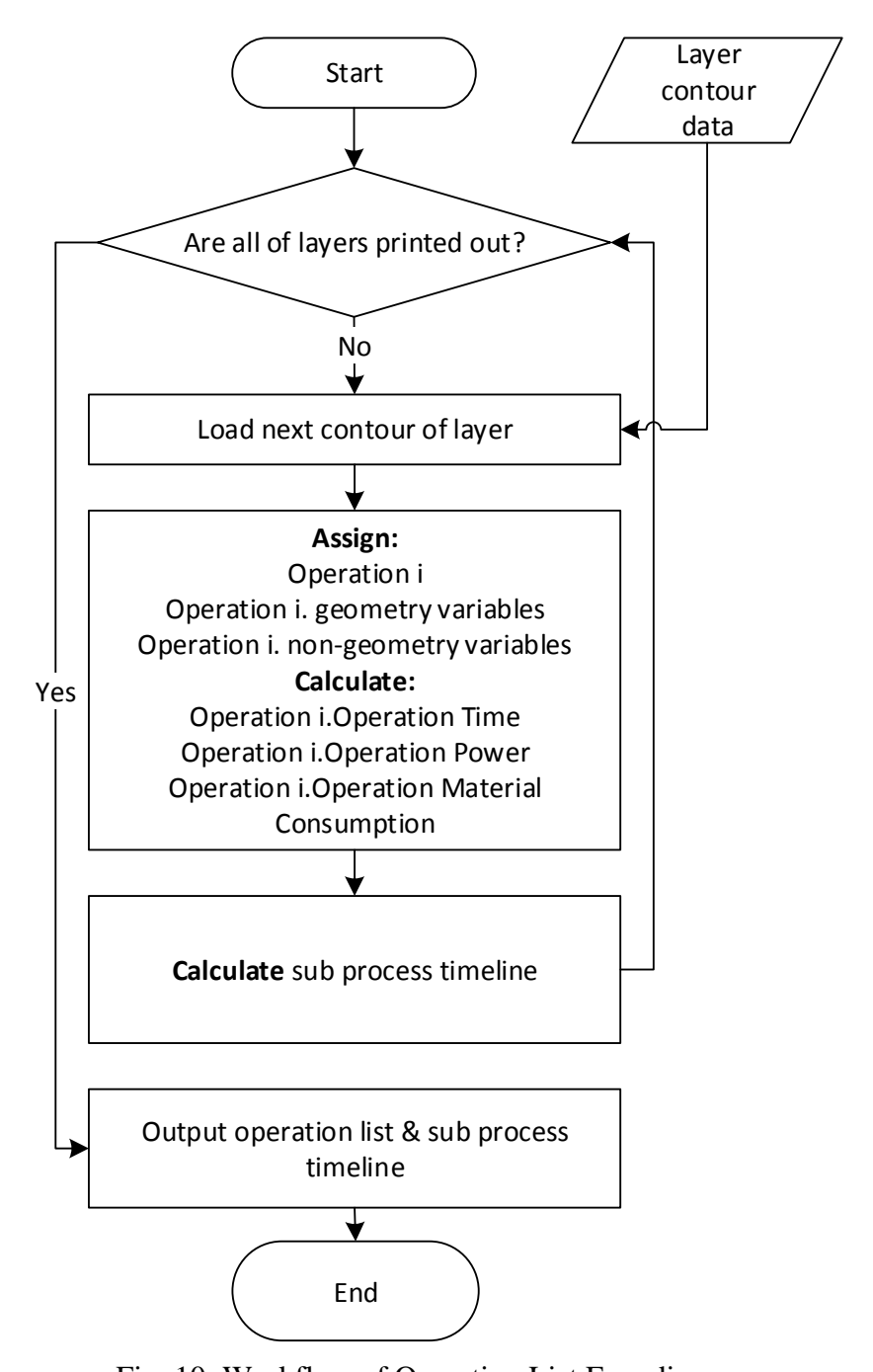


Fig. 10: Workflow of Operation List Encoding

The process of encoding can be seen as a simulation of a virtual AM process. As shown in Fig. 10, the structure of encoding program is a loop. In each iteration of the loop, the task is to print out the designed layer contour of the part. The printing process of a layer is decomposed into basic operations. The decomposition is based on the IDEF0 method which has been introduced in the first chapter. Different AM technologies are decomposed into different basic operations by the IDEF0 analysis. Then, the layer contour information and the process variables are input to the basic operations to

calculate the operation time, power and material consumption. When the virtual printing of one layer is finished, the basic operations are added into the operation list and the printing of the next layer start, which coheres with the real manufacturing process of AM.

# 3.4 Method of Part Slicing

The encoding program in section 2.3 requires the information of layer contours. This information is used as the geometry variables for the basic operations. In order to provide this information of layers, a part slicing program was developed in this research to slice the part. The workflow of the program is shown as Fig. 11.

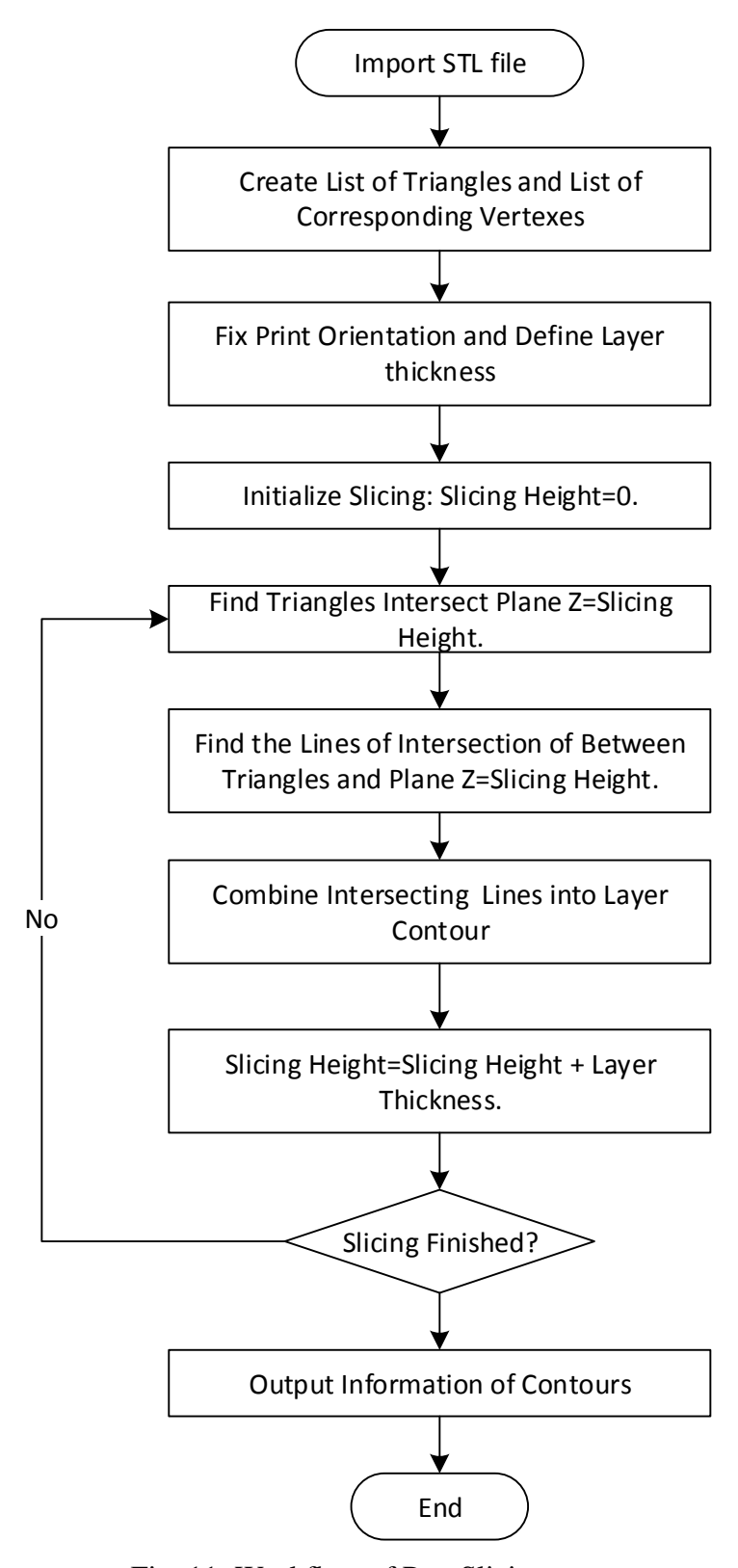


Fig. 11: Workflow of Part Slicing

Firstly, the geometry information of the part is derived from the STL file by a STL reader. Then the print orientation and layer thickness are defined by the user. These two process variables have significant influences on the total print time and printing quality,

which will be discussed in chapter 4. After part geometry, print orientation and layer thickness are presented, a slicing loop is performed to slice the parts into layers which are perpendicular to the print orientation. When the slicing is finished, the information of the contours is output to support the energy and material consumption. The details of the STL reader and slicing loop are demonstrated as following.

#### 3.4.1 STL File Reader

The functions of the STL file reader are to read the triangles from a STL file and generate two lists to save these data: the facet list and vertex list. As discussed in Chapter 1, both of the ACSII STL and Binary STL file have a section to save the data of triangles. In these sections, when a normal vector of a triangle appears it is always following by three vertexes of the triangle. According to this rule, when the STL reader read a normal vector in the STL file, a new triangle will be added into the facet list. Then the following three vertexes are added into the vertex list which is corresponding to the triangle list. The structure of these two lists are shown as following:

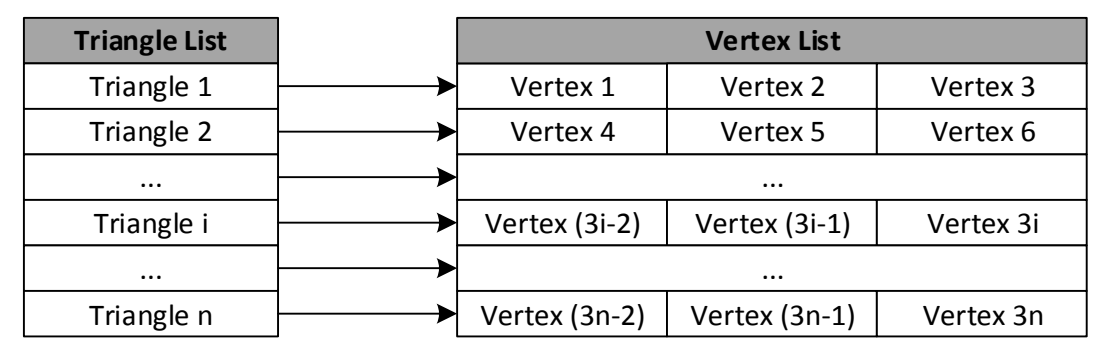


Fig. 12: Structure of Triangle List and Vertex List

If the part is represented by n triangles in the STL file. Then the triangle list is an  $n \times 1$  array while the vertex list is a  $n \times 3$  array. Fig. 12 shows the triangles list is used as an index list to find the elements in the vertex list.

## 3.4.2 Identify Intersecting Triangle

Once the STL is read into the program, the following task is to slice the part into layers and find out the intersections. As the slicing is conducted along the Z axis, the

first step is to find out the triangles intersecting the plane  $Z = Z_{Slice}$  where  $Z_{Slice}$  is the slice height. The test of intersecting can be performed as following:

In order to perform the intersecting check, a top and bottom vertex list of triangles are introduced. This list is a  $3 \times n$  array. The structure of the list is shown in

Fig. 13.

Triangle	1	2		3		3
Top Vertex	(X,Y,Z)top.1	(X,Y,Z)top.2	•••	(X,Y,Z)top.i	•••	(X,Y,Z)top.n
<b>Bottom Vertex</b>	(X,Y,Z)bottom.1	(X,Y,Z)bottom.2	•••	(X,Y,Z)bottom.i	•••	(X,Y,Z)bottom.n

Fig. 13: Structure of Top and Bottom List

The first row of the list saves the index of triangles. The second row saves the coordinates of the top vertex corresponding to the triangles and the third row saves the coordinates of the bottom vertex.

#### As shown in

Fig. 14, there are eight possible position relations between triangles and the slicing plane.

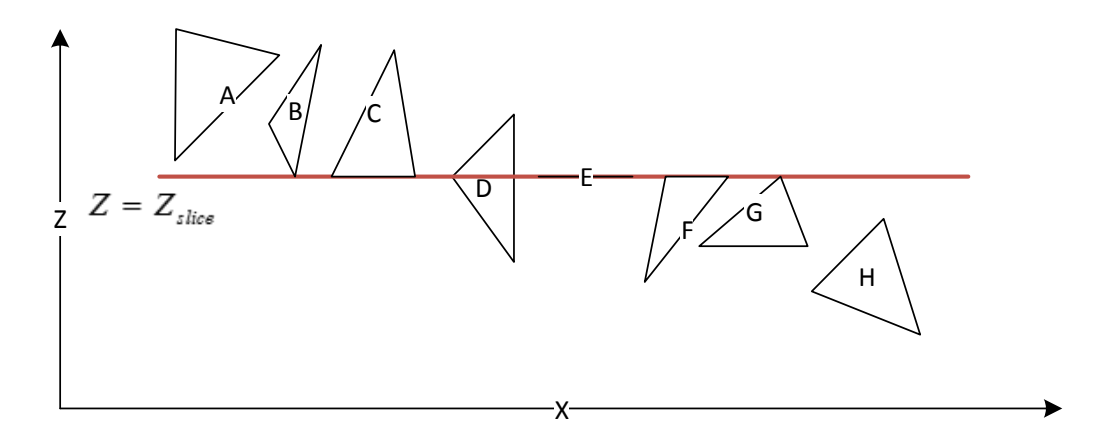


Fig. 14: Possible Position Relations between Triangles and Slicing Plane
The condition of intersection can be expressed as:

$$Z_{top.i} \ge Z_{slice}$$
 , Eq. 14 and  $Z_{hottom.i} \le Z_{slice}$  .

By program, the intersecting triangles are sorted out by the two operations below:

1. Add any triangles with  $Z_{bottom.i} \leq Z_{slice}$  from the top and bottom list into the intersecting triangle list.

2. Remove any triangles with  $Z_{top.i} < Z_{slice}$  from the intersecting triangle list.

Therefore for the example shown in the

Fig. 14, the first step adds triangle [B C D E F G H] into intersecting list. And the second step removes [H]; as a result, triangle [B C D E F G] are tested for intersection.

# 3.4.3 Calculate Intersection on Slicing Plane.

The intersection between a triangle and a plane is a segment. This segment can be located by finding out the two end points. Firstly, a test is performed to check if the vertexes of the triangles are on the slicing plane. If a vertex is on the plane, then it is one of the end points. This test can save the computation work and speed the program up. The conditions are discussed as following:

- 1. There is a vertex on the slicing plane and the rest of the triangle is above or below the plane (as triangle B or G in
- 2. Fig. 14). Under this condition, the whole intersection is a point and it is not computed.
- 3. There is a vertex on the slicing plane and the slicing plane is intersecting one side of the triangle (as triangle D in
- 4. Fig. 14). In this case, the vertex on the plane is one of the end points of the intersection segment.
- 5. Two vertexes of triangle are on the slicing plane (as triangle C and F in
- 6. Fig. 14). In this case, a side of the triangle is on the plane and it is directly treated as the intersection.
- 7. All of the three vertexes of triangle are on the slicing plane (as triangle E in
- 8. Fig. 14). Then the three sides of the triangle are all treated as intersection.

Other than the four situations, for any segment of the triangle with vertex on the both side of the slicing plane (shown as Fig. 15), the intersection point is computed as:

$$X_i = \frac{(Z_{slice} - Z_1) \cdot (X_1 - X_2)}{(Z_1 - Z_2)} + X_1.$$
 Eq. 15

Similarly:

$$Y_i = \frac{(Z_{slice} - Z_1) \cdot (Y_1 - Y_2)}{(Z_1 - Z_2)} + Y_1.$$
 Eq. 16

After the end points of the segment of intersection being computed, the segment of intersection is located.

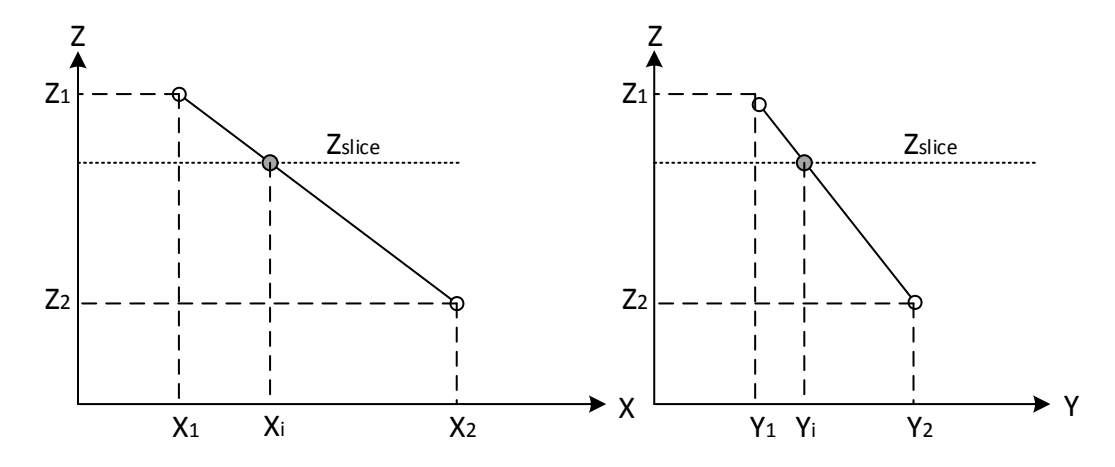


Fig. 15: Computation of Intersection Point

This process is performed iteratively for all of the intersecting triangles. As a result, the segments of the whole layer are derived and they are combined together to form the contour of the layer.

# Chapter 4: Modelling of BJ manufacturing process

In Chapter 2, a simulation method is proposed to calculate the power and material consumption of AM technologies. In this section, the proposed method is applied on the BJ technology. IDEF0 approach is employed to identify the basic operations of the printing process of BJ. Characteristics of operation power and operation time of the basic operations are analyzed. Also A power data analyzing system is proposed to provide the power data for the simulation. The detail of the above works are as following.

### 4.1 IDEF0 Analysis of BJ Process

By IDEF0 method, the BJ manufacturing process are decomposed as following:

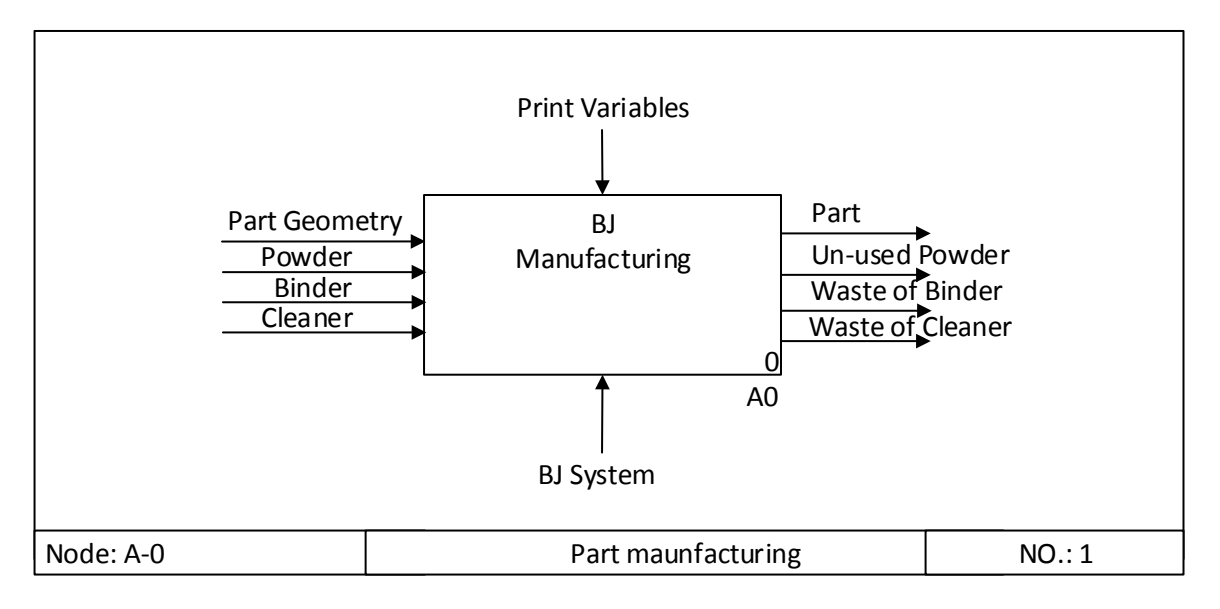


Fig. 16: Activity A-0

The analyzing starts with the A-0 level of the IDEF0 diagram. On this level, the whole BJ process is seen as one activity. The manufacturing is performed by the BJ printer, transform the CAD design and raw materials into part. This process is controlled by the process variables. This diagram defined the inputs, output and control of the BJ process explicitly. However, there is no information about the printing process of the BJ. Thus, more details of the manufacturing process are needed and the decomposing continues.

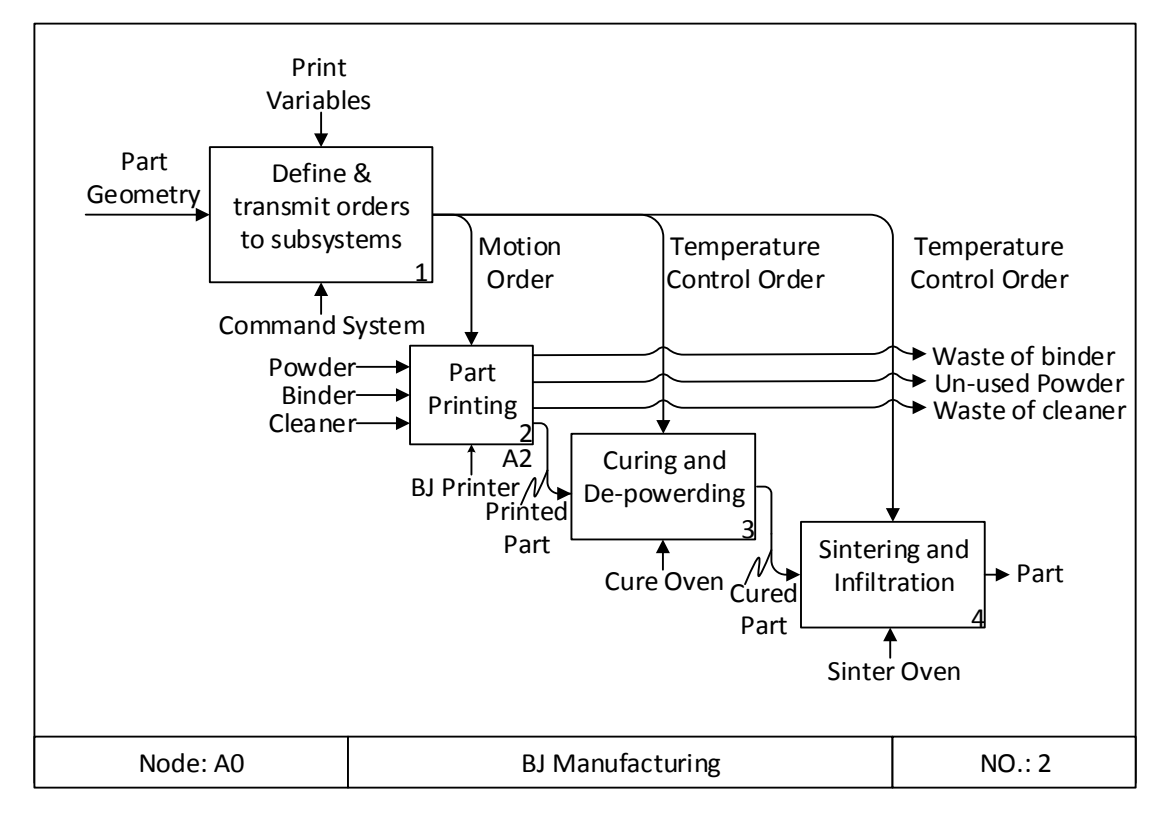


Fig. 17: Activity A0

By decomposing the A0 activity in Fig. 17, the whole manufacturing activity of BJ is decomposed into four activities: controlling of BJ process, part printing, curing and depowdering and sintering and infiltration. As this research concerns the printing process, again, the activity A2 (Part Printing) is decomposed.

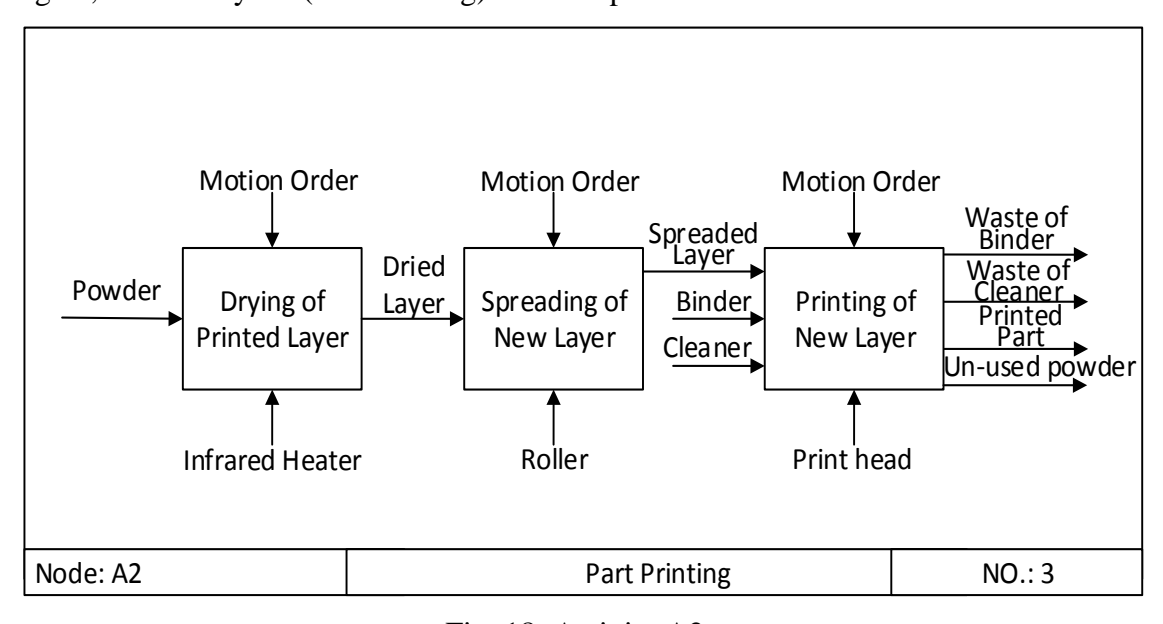


Fig. 18: Activity A2

In Fig. 18, the printing process is decomposed into three operations: drying of printed layer, spreading of new layer and printing of new layer. As an AM technology, BJ

fabricates part layer by layer. Based on this characteristic, all of the printing process of BJ can be seen as a repetition of these three operations. Thus, any part printing process of BJ can be represented by a combination of drying, spreading and printing. As mentioned in Chapter 2, when this criterion is satisfied, the decomposing stops and the three operations and defined as basic operations of the printing process.

# **4.2 Basic Operations of BJ Process**

Since the three basic operations of the printing process are identified, the characteristics of them are discussed here. This analyzing contributes to understanding how the basic operations consume the energy and materials. Also, it shows the influence of the process variables on the basic operations. The analyzing is as below.

# **4.2.1 Drying of Printed Layer**

After each layer being printed out, the binder needs to be dried by a heater to solidify. Otherwise, the binder may diffuse into other ares of the print bed through the space between powders and form un-desired layer shape. Also excessive binder is removed by the drying process. For the drying process, the print bed moves under beneath a dryer (shown as Fig. 19) to heat the binder and evaporate the undesired binder.

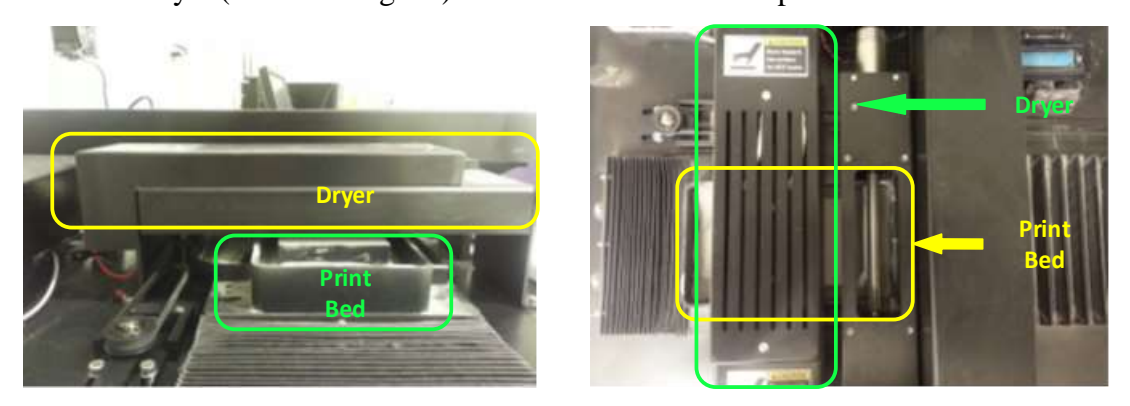


Fig. 19: Drying System of BJ printer

The only consumption of this process is electrical energy which consumed by the dryer. Therefore, the variables which decide the energy consumption are the power of dryer and the drying duration. Empirically, higher dryer power and longer drying duration can improve print quality. However, they will also increase energy

consumption and waste heat emission. To get a balance between print quality and energy performance, these two parameters need to be selected discreetly.

# 4.2.2 Spreading of New Layer

After drying, the print bed lower and the feed bed rise. Then, a roller evenly spread powder from the feed bed to the print bed. The spreading syste is shown as Fig. 20.

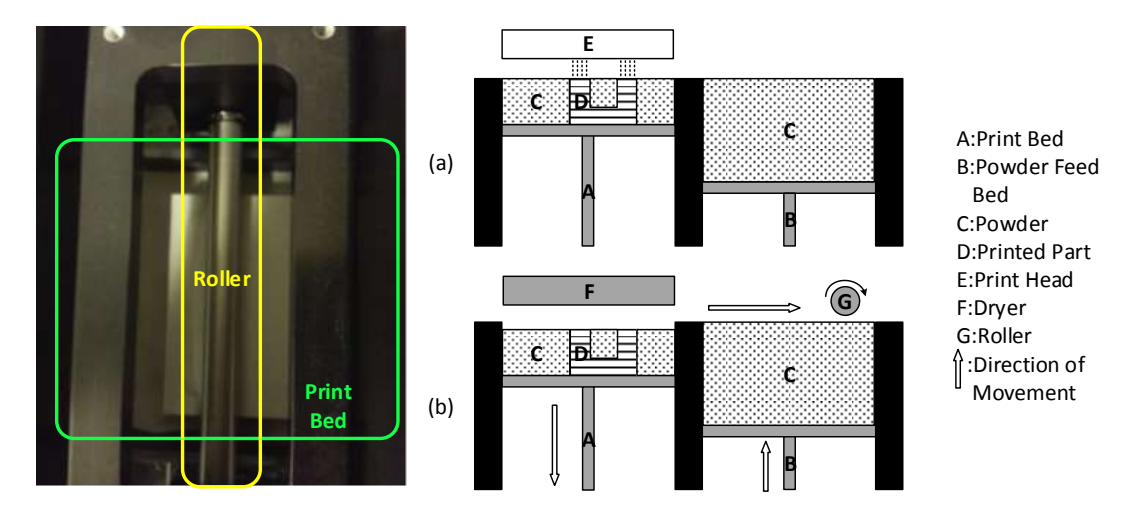


Fig. 20: Spreading system of BJ printer

The function of spreading system is to generate a new layer over a printed layer. This process can be seen as a preparation of the following printing process. The spreading is conducted by a roller and a belt system. As shown in Fig. 20, during the spreading, the roller is rotating and the belt system slowly traversing under the roller. Similar to the drying process, the only consumption of spreading is electrical energy. The energy consumption is determined by power and duration. Furthermore, the duration is determined by the spreading speed which defined by the user.

## 4.2.3 Printing of New Layer

The printing of part is realized by slicing the part into layers and print it out layer by layer. Thus, from this point, the printing of layers is the core operation of the printing process of BJ. For each layer's printing, the first task is to achieve the layer contour and send this information to the control system of the BJ printer. Then this control system generates commands to move the printhead and deposit binder drops on the print bed to form the layer contour. Another operation performed by the control system is to clean the printhead periodically. Which means after certain layers' printing, the nozzle of

printhead will be flushed by binder and a cleaning fluid (also called cleaner) is used to clean printhead. As the result, for the layer printing, both energy and materials are consumed. The energy consumption is the electrical energy while the material consumption is powder, binder and cleaner.

## **4.3 Operation Time of Basic Operations**

The former section analyzed the characteristics of the three basic operation: drying of printed lay, spreading of new layer and printing of new layer. Based on these analyses, the operation time of the three basic operations is discussed here. The operation time is determined by their form of motion. Three equations are derived by analyzing their motion in the following sections.

# 4.3.1 Drying of Printed Layer

The operation time  $t_d$  of the drying is a non-geometry variable which is defined by the user of the 3D printer. The duration of drying can be different from layer to layer. Up to now, there is still no mathematical relationship between the drying time and print quality. However, as mentioned in the former section, a relatively long operation time (50 seconds per layer or longer) is applied to ensure the quality of the first ten layers' printing. Then the drying time can reduce gradually (30 seconds per layer after the first 20 layers' printing) as the whole printing process generates heat and the temperature inside the printer has increased.

# 4.3.2 Spreading of New Layer

The spreading process aims to create a new layer of powder above the printed layer. Spreading is conducted by moving the print bed along X axis (as shown in Fig. 21).

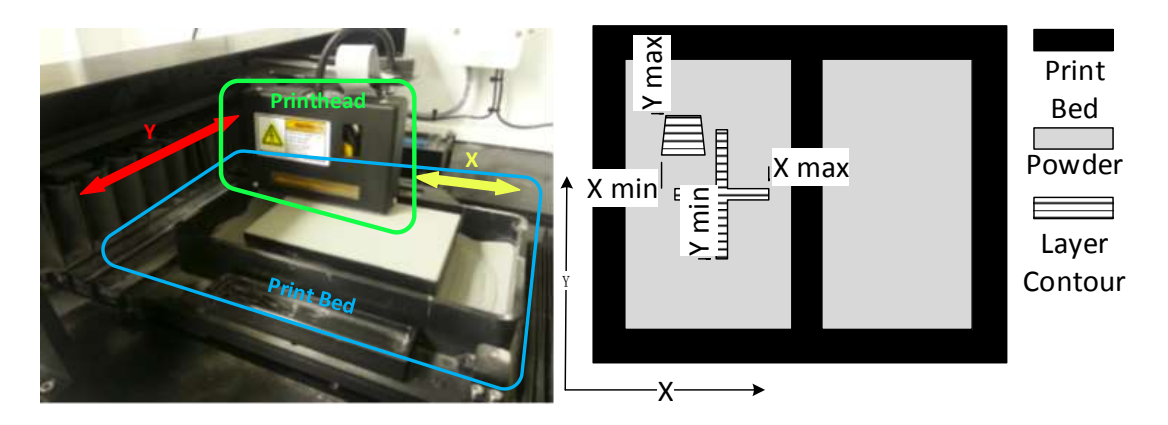


Fig. 21: Schematic of Print Bed

When the print bed moves under the roller. The powder is spread from the feed bed to the print bed. There are two speeds for the motion of the print bed: the spreading speed  $V_s$  and spreader rapid traversing speed  $V_{rs}$ . These two speeds are non-geometry variables defined by the user. The motion of the print bed is as following: The spreading is conducted under rapid traverse speed at the beginning. When the roller arrives  $X = X_{max} + X_{right}$ , it switches to slow spreading mode until roller arrives  $X = X_{min} - X_{left}$ ; The  $X_{left}$  and  $X_{right}$  are the left and right spreader rapid traverse border respectively. Then it switches back to fast spreading mode and traverse to the left end of the print bed. The X respects to time is illustrate as figure below:

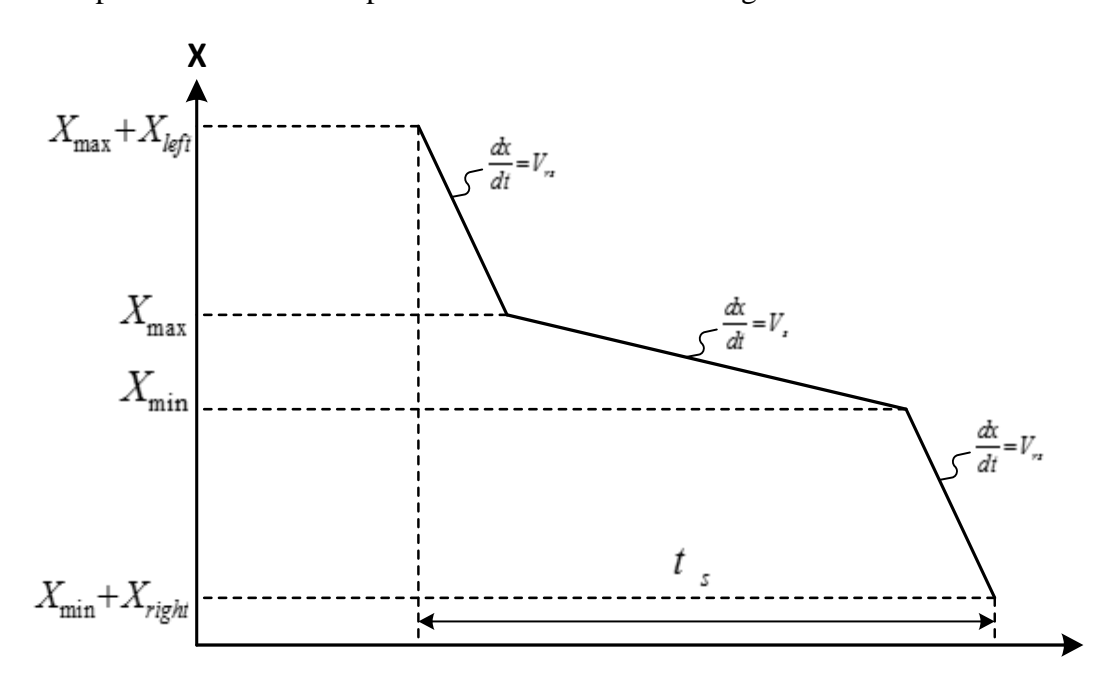


Fig. 22: Motion of Spreading

The operation time of new layer spreading  $t_s$  is calculated as:

$$t_s = \frac{(X_{left} + X_{right} + X_{max} - X_{min})}{V_s} + \frac{120 - (X_{left} + X_{right} + X_{max} - X_{min})}{V_{rs}}$$
 Eq. 17

Also geometry variables have influence on the spreading time. That are the minimum value and maximum value of X of the layer contour  $X_{min}$  and  $X_{max}$  respectively.

## 4.3.3 Printing of New Layer

In the printing process, the printing motion is achieved on the Y axis (shown as the red direction in Fig. 21). The printhead moves along the Y axis and deposit binder droplets on the powder bed according to the intersection of the part at each layer, which is similar to inkjet printer. The motion of the printhead is controlled by a belt system and this system is driven by a step motor. Since the step motor can start and stop immediately, the acceleration and deceleration of printhead are negligible. There are two patterns of the printhead motion: while moving on the positive direction of the Y axis, it is a uniform motion with speed of  $V_{printhead}$ ; while moving on the negative direction of the Y axis, it is a uniform motion with speed of  $-V_{printhead}$ .

The range of the motion is determined by contour of the intersection. Fig. 21shows an example of layer contour during the printing process. While printing, the printhead moving forward and backward along the Y axis. For each time of moving, the printer will wipe the printhead first. This process is a preparation of printing. Then it starts from Y = 0 and stops at  $Y_{max}$ . Then, it moves between  $Y_{min}$  and  $Y_{max}$  several time to deposit enough binder on the powder bed. As a result, the operation time of printing is determined by the geometry variable: the maximum value and minimum value of Y of the intersection contour. The correlation between them are expressed as:

$$t_p = 2n \cdot \frac{Y_{max} - Y_{min}}{V_{printhead}} + t_0$$
 Eq. 18

Where:

 $t_p$  is the operation time of printing (s),

 $Y_{max}$  is the maximum value of Y (mm),

 $Y_{min}$  is the minimum value of Y (mm),

n is the number of repetitions,

 $t_0$  is the time of preparation (s).

However, for the printing process, the number of repetitions n, time of preparation  $t_0$  and the speed of printhead  $V_{printhead}$  are constant. Thus, the term  $\frac{2n}{V_{printhead}}$  can be donate as a constant A while  $t_0$  can be donated as a constant B. Substitute A and B into Eq. 18, it can be re-written as

$$t_p = A \cdot (Y_{max} - Y_{min}) + B . Eq. 19$$

This equation is used as the principle of regression for the printing operation time in the latter section.

## **4.4 Material Consumption of Basic Operations**

There are three material consumables in the printing process of the BJ technology: powder, binder and cleaner. The binder is a mixture of ethylene glycol monomethyl ether and ethylene glycol, while the chemical component of the cleaner is ethylene glycol monobutyl ether (provide by © 2012 ExOne). The way the materials being consumed are discussed as below.

#### 4.4.1 Consumption of Binder

The function of the binder is to bind the steel powder together and form the designed shape. As shown in Fig. 23, during the printing, the binder is deposited on the steel powder by the printhead according to sliced layer contour.



Fig. 23: Contour of Slice

Therefore, the consumption of the binder is correlated to the shape of the layer contour. More specifically, it is correlated to the area of the layer contour. A more detailed numerical analysis of the binder consumption of printing is presented following section 3.4.2.

[photo of the layer contour, will be taken during the next sample printing]

On the other hand, the binder is also used as a fluid to flush the nozzle of the printhead. For each time of the flushing, 4000 drops of the binder are used. Therefore, the usage of binder also depends on the times of flushing. Furthermore, the times of flushing are determined by the "Flushing Frequency" (FF). This term refers to the time of flushing for each layer's printing and it is a process variable which defined by the user. For a specific printing process which has n layer to print out, the time of flushing operation  $N_f$  can be calculated as:

$$N_f = n \cdot FF$$
. Eq. 20

Then, the usage of the binder which used for the nozzle cleaning is calculated as:

$$C_{binder.c} = N_f \cdot B_c,$$
 Eq. 21

where  $B_c$  is the binder consumed by one time of flushing.

Eq. 21 is used to simulate the binder usage of cleaning process.

# 4.4.2 Printing Saturation

Printing Saturation (PS) is an important non-geometry variable which has significant influence on the binder consumption. The definition of PS is illustrated as following:

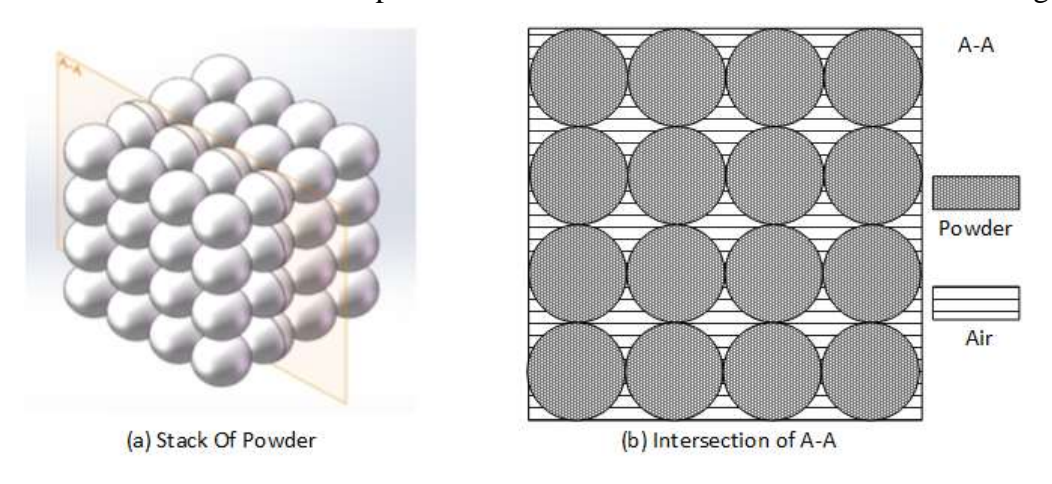


Fig. 24: Scheme of Powder Packing

The BJ technology works with a spherically shaped in-dissolvable powder. As shown in Fig. 24, when the spherical powders are stacked together, the gap between the powders is fill by air. The term "Packing Rate" (PR) is introduced here. It refers to the volume fraction of powder in a given volume of powder and air. For instance, given a material with a density of 1 unit mass per 1 unit volume. Then if 1 unit of volume of this material as a powder weighs 0.5 unit of mass, which means the PR of the powder is 50%. Therefore, the PR is defined as following equation:

$$PR = \frac{V_{powder}}{V_{solid}} = \frac{V_{solid} - V_{air}}{V_{solid}},$$
 Eq. 22

where:

 $V_{powder}$  is the volume of the powder;

 $V_{air}$  is the volume of the air;

 $V_{solid}$  is the volume occupied by the mixture of powder and air.

Assume the shape of the steel powders is identical and they are stacked in a perfect cubic-face arrangement (as shown in Fig. 24), the PR would be  $\frac{\frac{4}{3}\pi r^3}{(2r)^3} = \frac{\pi}{6}$ , or approximately 52.4%. This result agrees with the data which provided by the supplier of the BJ printer (© 2012 ExOne) that the material systems have a PR of values between 50% and 60%.

Define the PR in this way allows us to define the PS. PS is the percentage of air space that is occupied by the binder. Thus:

$$PS = \frac{V_{binder}}{V_{air}},$$
 Eq. 23

where:

 $V_{binder}$  is the volume of binder.

Combined with Eq. 22, Eq. 23 can be written as:

$$PS = \frac{V_{binder}}{(1 - PR)V_{solid}}.$$
 Eq. 24

As Eq. 24 is derived, now, a single equation which determine the usage of the binder can be written as:

$$V_{binder} = PS \cdot (1 - PR) \cdot V_{solid}$$
 Eq. 25

For the printing process of one layer,

$$V_{soild} = A_l \cdot t_l,$$
 Eq. 26

where:

 $A_l$  is the area of the layer contour;

 $t_l$  is the thickness of the layer.

As a result, combine Eq. 25 and Eq. 26 together, the binder consumption of one layer printing is derived as:

$$V_{binder} = PS \cdot (1 - PR) \cdot A_l \cdot t_l.$$
 Eq. 27

The binder usage of one layer printing then is present as a function of three variables: the PS, layer thickness and the area of the layer contour. The binder consumption of printing process is modelled based on this function.

As a result, combined Eq. 21 and Eq. 27, the total binder consumption of part printing is:

$$C_{binder.c} = C_{binder.c} + C_{binder.p} = N_f \cdot B_c + PS \cdot (1 - PR) \sum_{i=1}^{n} A_{l.i} \cdot t_l$$
, Eq. 28

where:

n is the number of layers been printed out.

 $A_{l,i}$  is the area of i th layer.

#### 4.4.3 Consumption of Cleaner

The binder has a risk to block the nozzles of the printhead during printing. To ensure the function of the printhead, a cleaning system is built in the BJ machine. The cleaner of the cleaning system is a watery solution of ethylene glycol monobutyl ether which has a concentration of 10%. It can dissolve the binder which used in the printing process. Therefore, this solution is used in the cleaning system of the BJ technology to clean the nozzles of the printhead.

To model the total usage of cleaner for a part printing, the term "Clean Frequency" (CF) is introduced. CF is a non-geometry variable which defined by the user. It refers to times of cleaning operations for one layer' printing. For instance, if the value of CF is 0.5, it means clean operations will conduct automatically after every two layers'

printing. The usage of cleaner for each cleaning process is fixed. Therefore, the total consumption of the parting printing is determined by the value of CF as Eq. 29:

$$C_{cleaner} = (n \cdot CF) \cdot C_c,$$
 Eq. 29

where  $C_c$  is the binder consumed by one time of cleaning.

# 4.4.4 Consumption of Powder

The powder is the material which used to form the designed part. The material of the powder could be stainless steel, glass or ceramic. For the BJ technology, the consumption of powder is made up of two components: the consumption to form the part and the wastage of the printing. Thus, the total consumption of powder is

$$C_{powder.t} = C_{powder.p} + C_{powder.w},$$
 Eq. 30

where:

 $C_{powder.t}$  is the total powder consumption.

 $C_{powder,p}$  is the powder consumption of part printing.

 $C_{powder.w}$  is the powder been wasted in printing.

During the printing, an inkjet like printhead moves across the bed of powder and selectively deposit the binder onto the powder according to the shape of the layer. Therefore, the consumption of powder of each layer's printing can be determined by the following equation:

$$M_{powder.i} = V_{powder.i} \cdot \rho_{powder} = A_{l.i} \cdot t_{l.i} \cdot \rho_{powder},$$
 Eq. 31

where:

 $M_{powder.i}$  is the mass of the consumed powder of i th layer;

 $V_{powder}$  is the volume of the consumed powder of i th layer;

 $\rho_{powder}$  is the density of the powder.

By Eq. 31, the powder consumption of each layer can be calculated, then the powder consumption of part can be derived by summing the powder consumption of each layer. Thus:

$$C_{nowder,p} = \sum_{i=1}^{n} M_{nowder,i},$$
 Eq. 32

where:

n is the number of layer been printed.

The wastage of the powder is due to the loss of powder during un-used powder collection. After the parting being print out, the un-used powder is collected for recycling. During the collecting process, certain percentage of the un-used powder will be lost. The percentage of the lost powder is a statistical result. Defining  $\varepsilon$  as the recycle percentage of powder, then we have:

$$\varepsilon = \frac{M_{recycle}}{M_{unused}},$$
 Eq. 33

where:

 $M_{recycle}$  is the mass of the powder been recycled;

 $M_{unused}$  is the mass of powder been.

Then, the wastage of powder is the difference between unused powder and recycled powder, which means:

$$C_{powder.w} = M_{unused} - M_{recycle},$$
 Eq. 34

For the un-used powder, as before each time of printing, the 40 x 60 x 35 mm feed box is fully filled by the fixed amount of powder. Therefore, the unused powder can be calculated as:

$$M_{unused} = M_0 - C_{powder.p},$$
 Eq. 35

 $M_0$  is the mass of the powder to fully fill the feed box.

Combine Eq. 33, Eq. 34 and Eq. 35 the wastage of powder can be derive:

$$C_{powder.w} = (1 - \varepsilon) \cdot (M_0 - C_{powder.p}).$$
 Eq. 36

Finally, substitute by equations above, the total powder consumption equation can be re-written as:

$$C_{powder.t} = \varepsilon \cdot C_{powder.p} + (1 - \varepsilon) \cdot M_0 = \varepsilon \cdot \sum_{i=1}^{n} M_{powder.i} + (1 - \varepsilon) \cdot M_0$$
. Eq. 37

The above equation is then used for the powder consumption analysis and simulation.

## 4.5 Method of Power Data Analyzing

After being decomposed into basic operations, the energy consumption of each individual basic operations is calculated separately. At this step, to support this calculation, the power and time data of the basic operations are needed. In order to provide these power and time data, a power analyzing system is employed in this research.

The input of the analyzing system is the experimental time-power curves of the manufacturing process of BJ while the outputs are the power data and operation time of basic operations. The workflow of the analyzing system which is used to process the experimental data is shown in the Fig. 25 below:

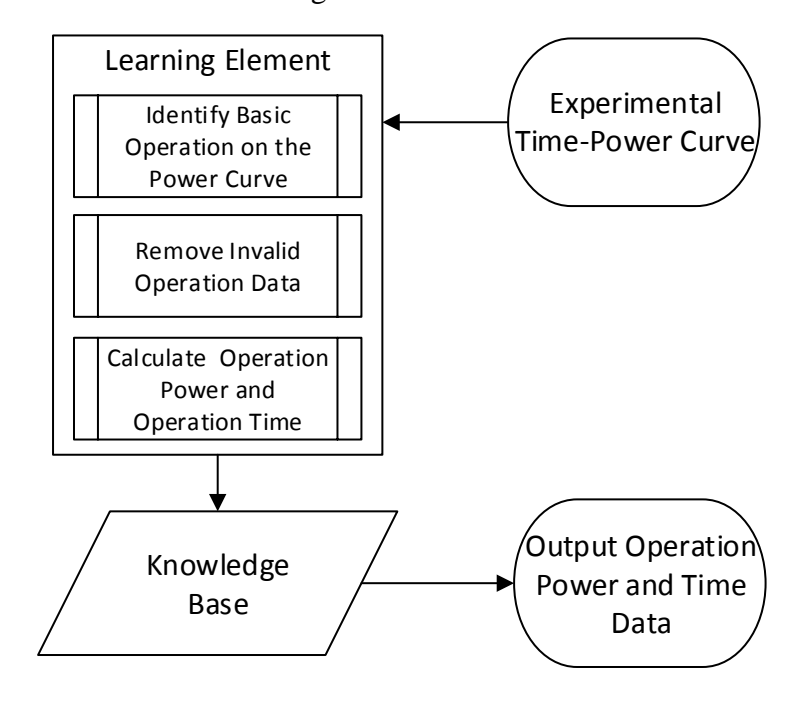


Fig. 25: Workflow of Power Analyzing System

The power analyzing method is made up of three components: the learning element, the knowledge base and the performance element. The workflow of this system is as following: firstly, experimental power data are input into the learning elements and been decomposed and analyzed. Then valid data are identified and saved into the knowledge base. While the energy simulation need data to conduct energy calculation, it will call data from the knowledge base and the performance element will pick the required data from the knowledge base and output them to support calculation. The details of the three components are demonstrated in the following sections.

## **Learning Element**

The learning element receives and analyzes the time-power curves which obtained from the experiments. It is also the core of the power curve analyzing system. Three tasks are accomplished by the learning element:

- 1. Identify basic operation on the time-power curves.
- 2. Remove invalid operation data: because of the noise, not all of the power signal can be used for analyzing. Therefore, invalid data should be removed to ensure the reliability.
- 3. Calculate operation power and operation time: statistical computations are performed on the valid power data to obtain the operation power and operation time.

The outputs of learning element are the operation power and operation time of the basic operations. These data are exported and saved in the knowledge base.

#### **Knowledge base**

The knowledge base is a database which saves the operation power and operation time data of basic operations. As new data are input by the learning element, knowledge base will update automatically to improve the data quality.

#### Performance element

The performance element is responsible for output data to the energy calculation program.

#### 4.5.1 Data analysis method of learning element:

As shown in Fig. 26, the discrete input data which measure by a power meter are made up of two arrays: the time and the power corresponding to the time.  $P_i$  is the i th element of the power data which sampled by the power meter at time  $t_i$ .

Power	P1	P2	 Pi	 Pn
Time	t1	t2	 ti	 tn

Fig. 26: Structure of Power Data

To analyze these data and extract information for basic operations, the following four steps are conducted:

1. Locate basic operations on the power curve.

- 2. Check the validity of located operations.
- 3. Process valid data by statistical computation.
- 4. Export and save data.

## **4.5.2 Locate Basic Operations**

The first task of analyzing the power data is to identify the basic operations on the power curve. In this research, the basic operations are located by the "edges" on the power curve. Fig. 27 shows an example of detecting edges on the power curve. Since the BJ machine only conducts one basic operation at a time, when the start time and end time of an operation are detected by the increase edge and decrease edge respectively, the operation is located on the power curve.

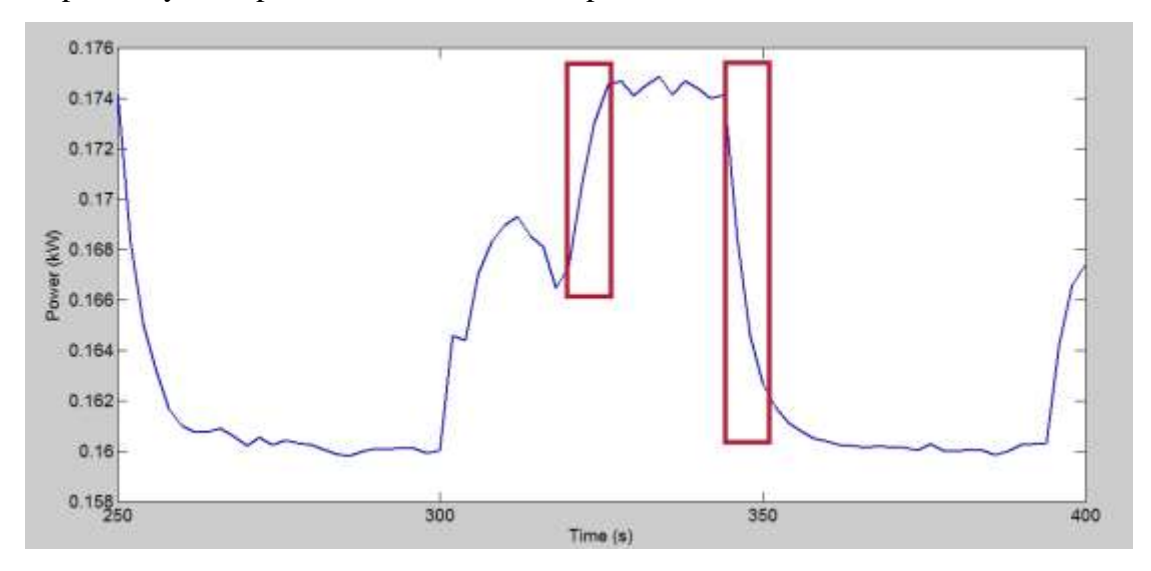


Fig. 27: Detecting Edges on Power Curve

By following steps, the basic operations on the power curve are located:

## Differentiate the power data

The edges on the power curve stand for fast increase or decrease of power. These changes are due to the switches of operations. According to the knowledge of differentiation, accompany with a sharp increase or decrease of the power curve, there would be a maxima or minima on the First Derivative of Power (FDP) curve respectively. Therefore, in order to detect the edges, the first derivative is calculated.

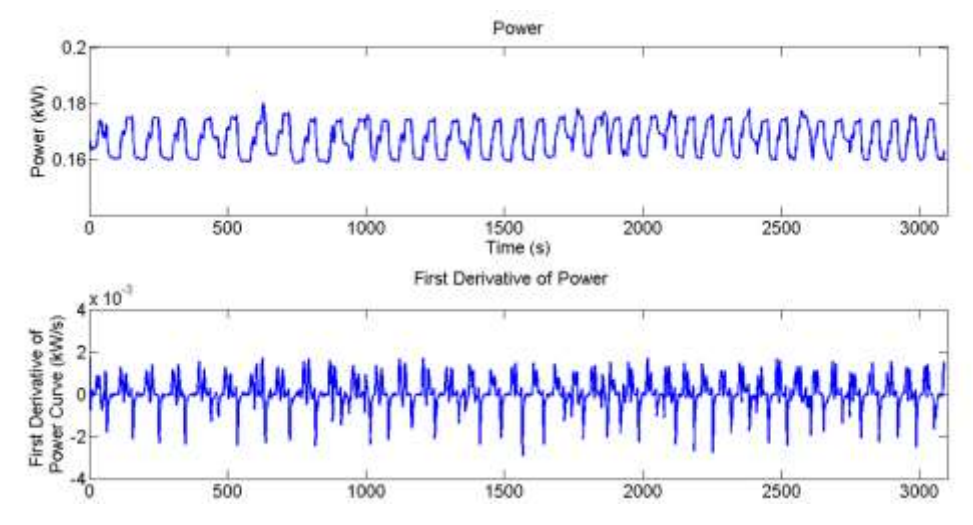


Fig. 28: Power Curve and Its' First Derivative

Fig. 28 shows an example of the power curve of printing process of BJ technology and its' first derivative. Considering the measured power data are discrete, the FDP are calculated as following:

$$\frac{dP}{dt_i} = \left(\frac{P_i - P_{i-1}}{t_i - t_{i-1}} + \frac{P_{i+1} - P_i}{t_{i+1} - t_i}\right) / 2,$$
 Eq. 38

where:

 $\frac{dP}{dt_i}$  is the i th element of FDP power corresponding to the time  $t_i$ ,

 $P_i$  is the i th element of power corresponding to the time  $t_i$ ,

 $t_i$  is the i th element of time array.

To improve the accuracy, the first derivative values are the average of the forward difference and backward difference. However, for the first and the last element of the first derivative, as there is no forward or backward element respectively, they cannot be calculated as Eq.1. Instead, we assume the first element of the first derivative equals to the second element while the last one equals to the second last one.

#### • Filter the FDP data

In Fig. 28, the sharp changes on the power curve are reflected by on the maximum or minimum peaks on the cure of FDP. However, the noise on the first derivative curve generates peaks which are not corresponding to edges of the basic operations. A Gaussian filter thereby is used to process the FDP data to remove the noise. Gaussian filter is a filter which has a Gaussian function impulse response. The advantage of Gaussian filter is it has the minimum possible group delay. This is due to its' properties

of having no overshoot to step function input and minimizing the rise and fall time.[37] Therefore, the Gaussian filter is an ideal tool to process the time versus power data which is a time domain signal.

Mathematically, the Gaussian filtering is conducted by convoluting the input data with a Gaussian function as following Eq. 39:

$$F(x) = \frac{1}{\sigma\sqrt{4\pi}} \int_{-\infty}^{\infty} f(y) e^{-\frac{(x-y)^2}{4\sigma^2}} dy,$$
 Eq. 39

where:

- f(x) is the input function,
- F(x) is the output function.

The Gaussian function is non-zero for  $[-\infty, \infty]$  and would theoretically require an infinite window length. However, since it decays rapidly, it is reasonable to truncate the filter window and implement the filter directly in a narrow window. Fig. 29 shows a result of filtering while  $\sigma = 2$  and the window length is  $[-5\sigma, 5\sigma]$ .

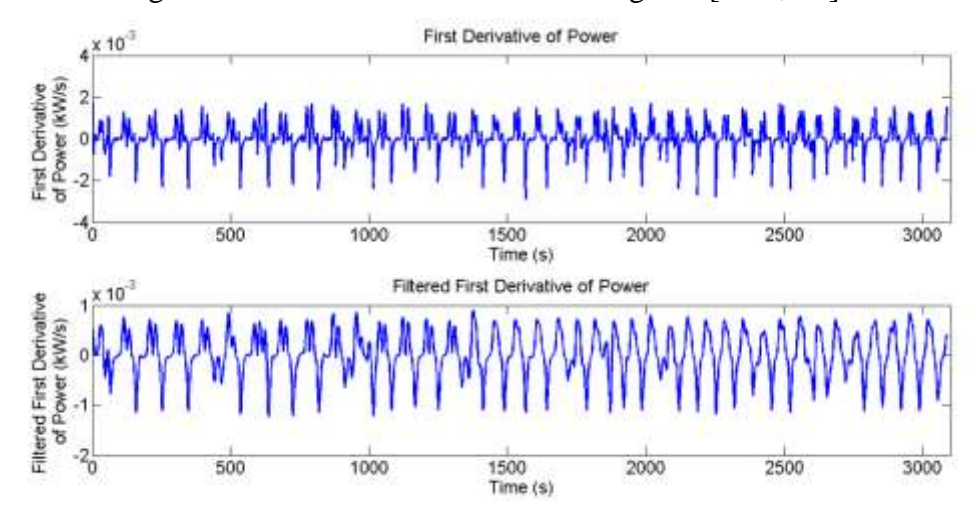


Fig. 29: Filtered FDP curve

As shown in Fig. 29, after being filtered by the Gaussian filter, the noise on the FDP curve is significantly reduced, which increase the accuracy of the following peak detecting.

## • Detect peaks on the filtered first derivative

Mathematically, the peak on a curve can be found by the following criterion:

If a function f(x) is twice differentiable on interval [a, b], with its' first derivative f'(x) and second derivative f''(x), while:

$$f'(x) = 0;$$
 Eq. 40

if f''(x) > 0, then f has a local minima at x; if f''(x) < 0, then f has a local maxima at x;

if f''(x) = 0, then the test is inconclusive and higher derivative test needs to be performed.

Applying the above test criterion on the filtered FDP data. Define FFDP' and FFDP' are the first and second derivatives of filtered FDP data with respect to time. Then the criterion above can be written as:

While

$$FFDP'(t) = 0;$$
 Eq. 41

if FFDP''(t) > 0, then the filtered FDP data has a local minima at t; if FFDP''(t) < 0, then the filtered FDP data has a local maxima at t; if f''(x) = 0, we consider this maxima or minima is flat and is not a peak.

Fig. 30 shows a peak detecting result by using this criterion. The peaks on the filtered FDP curve are correctly detected.

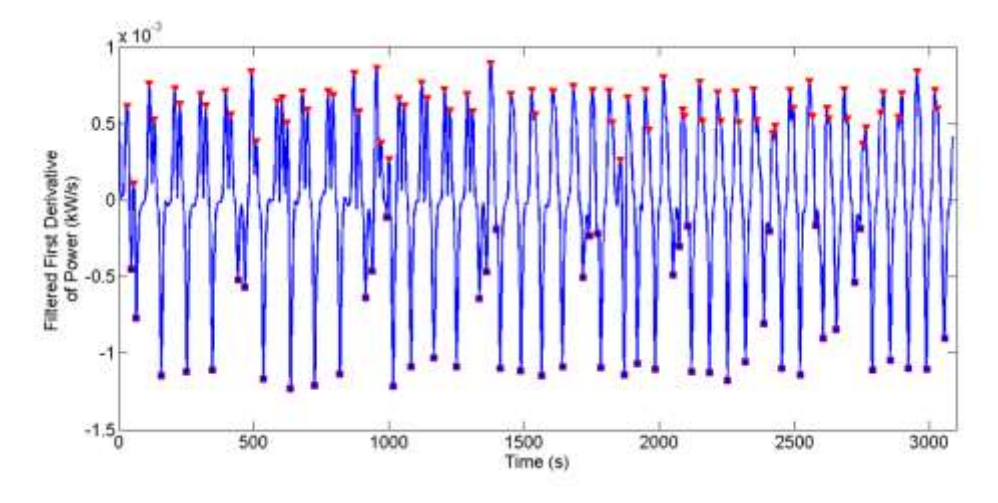


Fig. 30: Peaks on The Filtered FDP Curve

# Locate basic operations on power curve

When the peaks are detected on the filtered FDP curve, the time corresponding to these peaks are saved as an array  $tp_i$  and exported to locate the basic operations. By detecting the peaks, the time corresponding to the edges on the power curve is detected.

As mentioned before, the BJ machine only conducts one basic operation at a time and the basic operations are executed sequentially. Therefore, the edges can be used to divide the time interval of the basic operations on the power curve. Fig. 31 shows an instance of basic operations being located by the edges.

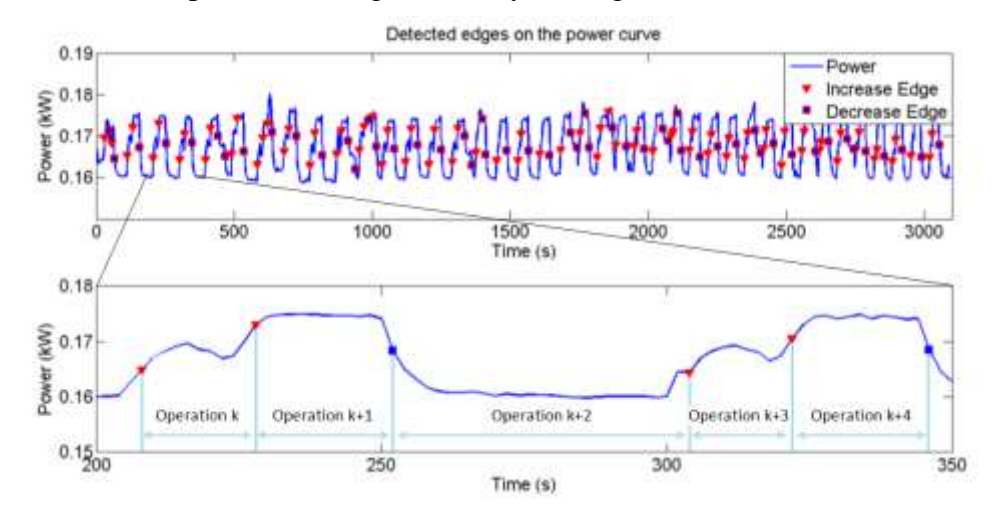


Fig. 31: Located basic operations

# **4.5.3 Validation of Located Operations**

As discussed before, the random noise on the power data will prevent the locating of basic operations. Even been filtered by the Gaussian filter, some of the data are still invalid and cannot be used for power analyzing, otherwise, the accuracy of the analyzing result will be reduced. Fig. 32 gives an instance of valid and invalid interval of the power data. For the valid data on the bottom left, it has a two-step stair like shape due to the power levels of three basic operations. On the contrary, the invalid interval of operations has a random shape. This shape characteristic is used to check the validity of the located operation intervals.

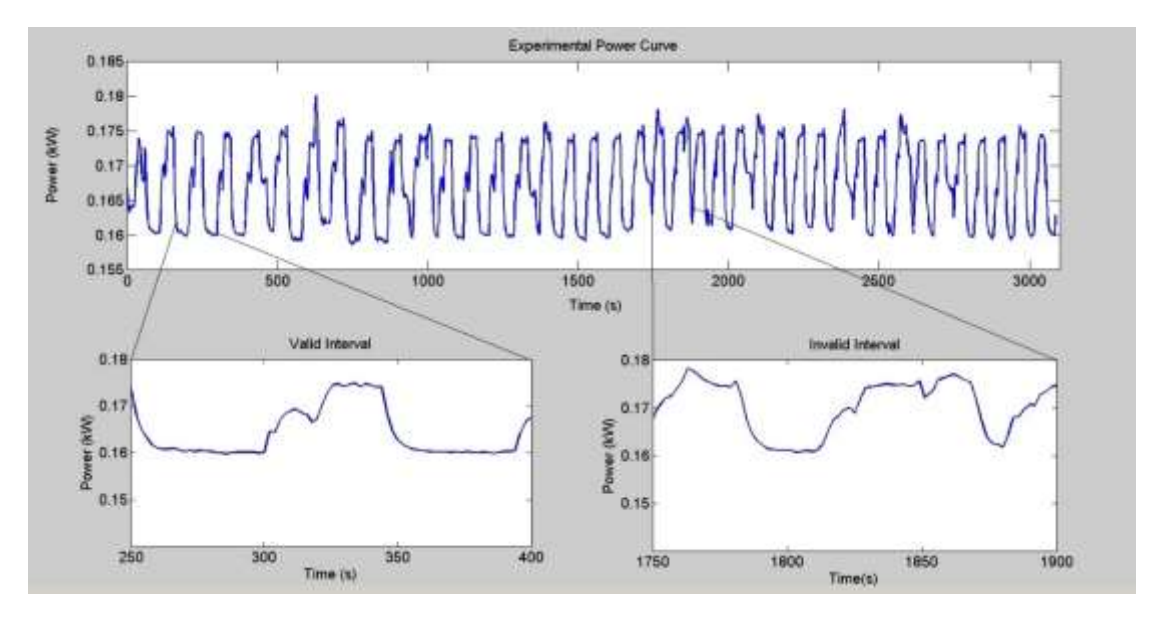


Fig. 32: Example of Valid Operation Interval and Invalid Operation Interval

## 4.5.4 Statistical Computation of Valid data

The function of the power data analyzing system is to provide the operation power and time data for the time and energy simulation. Therefore, during the analyzing process, these two kinds of data are collected and processed by statistical computation. The computation is performed as following:

## Average power calculation

The first step of the statistical computation is to calculate the average power of the valid operations. Since the time points corresponding to the edges on the power curve are saved as an array  $tp_i$ . They are also the start and end time of the operations on the power curve. For a valid operation which the start time  $t_{i.start} = tp_i$  and end time  $t_{i.end} = tp_{i+1}$ , The average operation powers are calculated as Eq.5:

$$\overline{P_i} = \sum_{k=start}^{end} P_k,$$
 Eq. 42

where:

 $\overline{P_i}$  is the average operation power of operation i;

 $P_k$  is the k th element in the power array;

*i. start* is the index of the time array where  $t_{i.start} = tp_i$ ;

*i.end* is the index of the time array where  $t_{i.end} = tp_{i+1}$ .

After the average power of all to the valid operations been calculated out,  $\overline{P}_t$  is saved as an array and exported for further analyzing.

# Cluster and identify operation type

Ignoring the operation for this moment, the calculated average operation powers are scatter plotted on a power-axis as shown in Fig. 33. These are then grouped into clusters by the DBSCAN clustering method. In Fig. 33, the average operation powers are divided into three clusters. Ideally, each cluster represents one kind of basic operation.

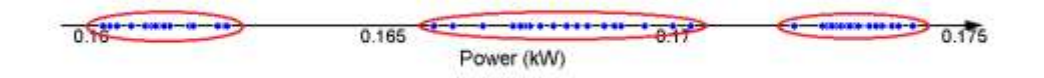


Fig. 33: Clustering of Operations

The data used to generate Fig. 33 were collected during a printing process of the BJ technology which is made up of three kinds of basic operations: drying, spreading and printing. As the high-to-low energy level of the three basic operations are printing, spreading and drying, the first cluster corresponds to drying, the second one corresponds to spreading and the third one corresponds to printing. Thus, by clustering the operation by power, the type of operation is identified. Then, statistical computations are performed on each cluster to achieve operation power and time data.

# Operation Power of Basic operations

After the basic operations being clustered and labelled with operation type, statistical computation is performed to achieve the power and time data of the basic operations. For the operation power, the mean value of each cluster is used as the operation power of the cluster (as Eq. 43).

$$P_l = \sum_{m=1}^{n} P_{l,m},$$
 Eq. 43

where:

 $P_l$  is the operation power of cluster l;

 $P_{l.m}$  is the m th element in the cluster l;

n is the number of element in the cluster l;

The reason of using the mean value is as below:

For the power measurement, the measured data are believed to have a normal distribution whose true value is at the center of the distribution. As the power of each operation is a function of the process variables and it will not change for one printing process. The data in a cluster can be seen as values of repeated measurement. Therefore, by taking the average value, the errors of each time of measurement can be offset and make the result converge to the true value.

## Operation Time of Basic operations

As discussed in the former section, the operation time of the drying and spreading are determined by the process variables. Therefore, regression is only adopted to the printing operation data. According to Eq. 19, the operation time and has a linear relationship with the value  $Y_{max}$  and  $Y_{min}$ , a linear regression are performed to achieve the constant coefficient A and B.

# 4.5.5 Saving Data in Knowledge Base

After the power analysis being finished, all of the results are saved in the knowledge. The structure of data in the knowledge base is as figure below:

Operation Type	Process Varibles	Operation Power	Operation Time
----------------	------------------	--------------------	----------------

Fig. 34: Structure of Data in Knowledge Base

There are two function of the knowledge base:

- Save the operation power and operation time data for a specific set of process variables. If a simulation is performed under this set of process variables, the knowledge will provide these data for calculation.
- 2. If another printing is conducted with a set of process variables which have been already recorded in the knowledge base, and the power data of the printing is analyzed. The knowledge base will update the operation data of this set of process variables with the mean value of the existed data and the new data. The reason to conduct this is because from the perspective of statistical the larger sample data can increase the precision.

# 4.5.6 Test Sample for Collecting Power Data

The power analyzing method discussed above can work with the existing time-power curve and derive the operation time and operation power information of the basic operations. However, if there is no existing data for a set of process variables of printing, a test sample will be printed and the power data will be logged and analyzed. The geometry of the test sample is shown in Fig. 35.

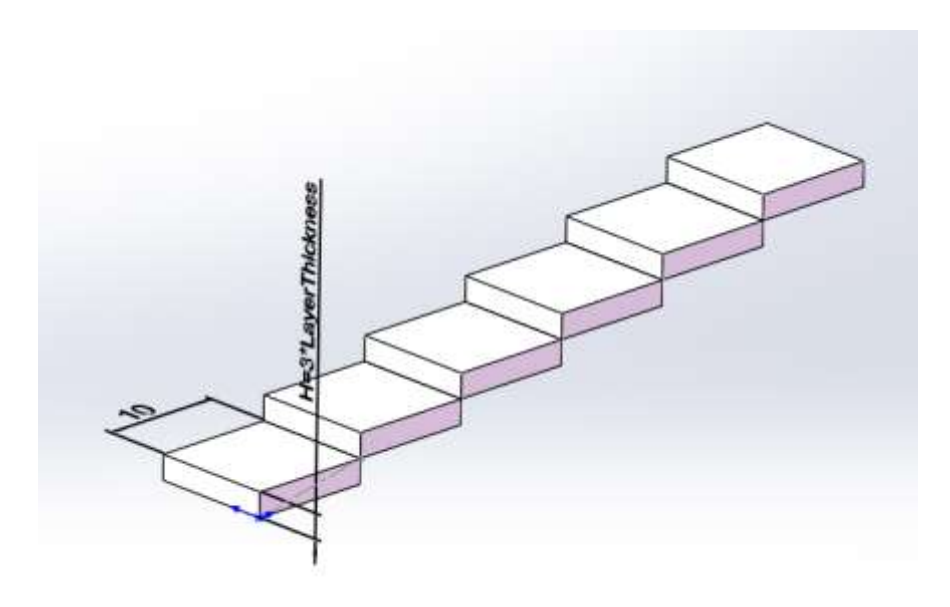


Fig. 35: Test Sample for Collecting Power Data

The test sample has a staircase shape with 6 steps. The length of each step is 10 mm. The reason to design such a staircase shape is to support the linear regression of the printing process. As each step of the stair has different  $Y_{max}$  and  $Y_{min}$  values, this shape provides data for the linear regression of the printing process. In order to save the materials and time, the thickness of each step is three times of the user defined layer thickness. Thus, each step is finished by three layers' printing, which ensures to get at least on valid operation data for each step.

# Chapter 5: Validation and Simulation of Test Case

In Chapter 3, a simulation method was developed to calculate the energy and material consumption for AM technologies. Afterward, Chapter 4 demonstrated how to apply this method on the BJ technology. IDEF method was used to decompose the printing process of BJ and identify the basic operations. Then, the characteristics of energy and material consumption of these basic operations were analyzed. Furthermore, as the simulation method requires power information to support the energy calculation, a power analyzing method for BJ process was developed in chapter 4 to provide these power data. After achieving the BJ model, validation and case studies are performed in this chapter.

The first objective of this chapter is to check the validity of the proposed simulation method and the BJ model. Driven by this objective, printing experiments are conducted and the energy and material consumption are recorded to perform the validation. After verifying the validity of the simulation method, a series of test cases are simulated to achieve the energy and material consumption features of the printing process of BJ. Parts with different geometry are simulated with different print orientation and process variables. The results of simulation show how the part geometry, print orientation and process variables influence the energy and material consumption. Based on the results of these case studies, features of the printing process of BJ are derived.

#### 5.1 Validation of BJ Model

For the BJ energy and material consumption simulation model, the inputs are the part geometry and process variables while the outputs are the energy and material consumption. To check the validity of simulation, the energy and material consumption of BJ technology is simulated with different set of inputs. Also, a series of experiments are performed with the same inputs. Both of the simulation model and the real printing system can be viewed as a transformation from inputs to outputs. Therefore, by comparing the output of simulation transformation to corresponding output of the real system

transformation with the same inputs, the validity of the simulation is checked. If these two outputs agree with each other with an acceptable error tolerance (the difference between them are not significant), the simulation model of BJ in this research is valid and can be used as a LCI analyze tool for part design and choosing of process variables for BJ technology. Otherwise, the simulation model of BJ is invalid and need to be calibrated.

The validation process is performed in two steps. For the first step, parts of different geometries are printed with the same process variables by the BJ printer. The time-power curves and material consumption of these printing process are recorded. Then, the recorded data are compared with the simulation result. If simulation results agree with the experimental data, then it verifies the simulation method can work with different part geometry.

In the second step, a part is printed with different process variables. Again, the experimental data are recorded and compared to the simulation result. If the results agree with the experimental data, it shows the simulation method can work with different process variables properly.

As there are only two kinds of input variables for the simulation: the part geometry and process variables, if the simulation model can calculate the energy and material consumption for different part geometry and process variables properly, then it is confident to say the simulation method can correctly simulate the energy and material consumption of BJ process (with certain error tolerance). Thus, the simulation method is valid. Otherwise, the simulation method and the model of BJ need to be checked step by step to find out where the mistake is and calibrated. Then, the validity will be checked again.

Before validation, basic parameters about the powder (stainless steel 420) and ExOne X-1 printer are listed in Table 1.

Table 1: Parameters of Powder and Printer

Parameter	Value			
Build Volume	40 x 60 x 35 mm			
PR of Powder	52.7 %			

Density of Powder	$4.071 \text{ g/cm}^3$
Binder Consumption of Flushing $(B_c)$	7.158 ml/time
Frequency of Flushing	0.5 time/layer
Cleaner Consumption $(C_c)$	6.24 ml/time

These parameters are treated as constant for the simulation. The details of the validation are as following:

# **5.1.1 Interface of Simulation Program**

A Graphic User Interface (GUI) of the BJ model is developed Matlab (The MathWorks, Inc) to simplify the input process of simulation. The main screen of the GUI is shown in

Fig. 36.

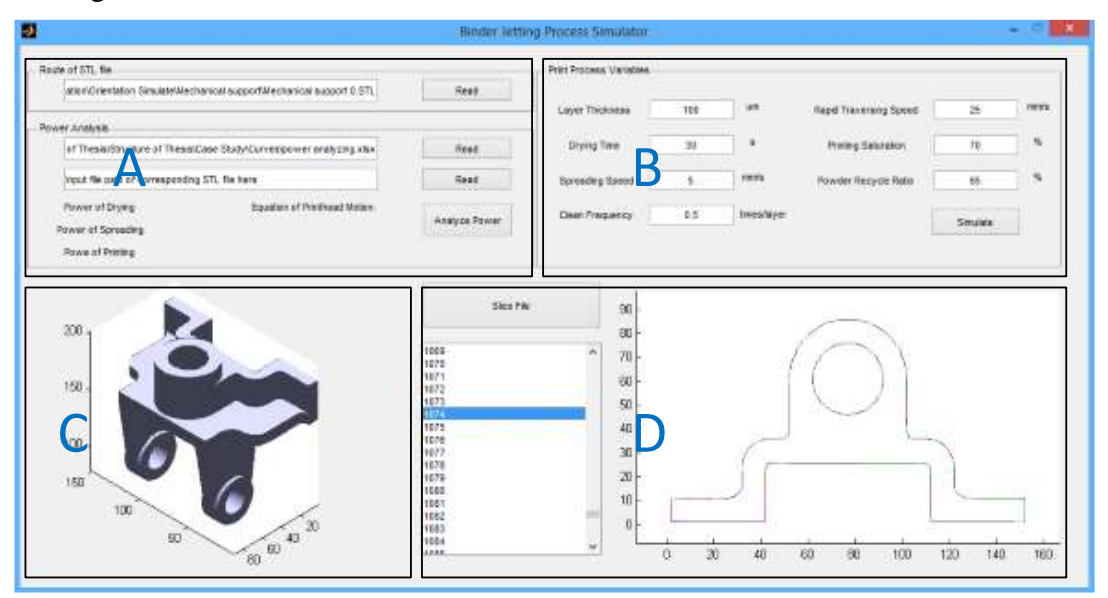


Fig. 36: User Interface of Simulation Program

The main screen is consist of 4 sections. The functions of the 4 sections are as following:

Section A: Section A is used to input files of part geometry and power data. It is
made up of two panels. The first panel reads the part geometry (in STL format) for
the energy and material consumption simulation. The second panel reads the power
curve and the corresponding learning part geometry for the power analyzing method.

- 2. Section B: By filling the blanks in section B, the process variables of simulation are defined.
- 3. Section C: After reading the STL file, the part geometry is exhibited in section C. User can have a quick review of the part.
- 4. Section D: The contours of slices are exhibited in section D. By clicking the layer number in the slice list, user can switch to different layers.

#### **5.1.2 Simulation of Different Part Geometries**

As aforementioned, firstly, parts of different geometries are printed with the same process variables to check if the BJ model can work with different geometry inputs. The following geometries of parts are printed for the test: a solid cylinder, a cylinder with cubic lattice structure, and cuboid with no-uniformed cubic lattice structure and möbius infinite strip. Fig. 37 shows the geometries of the parts.

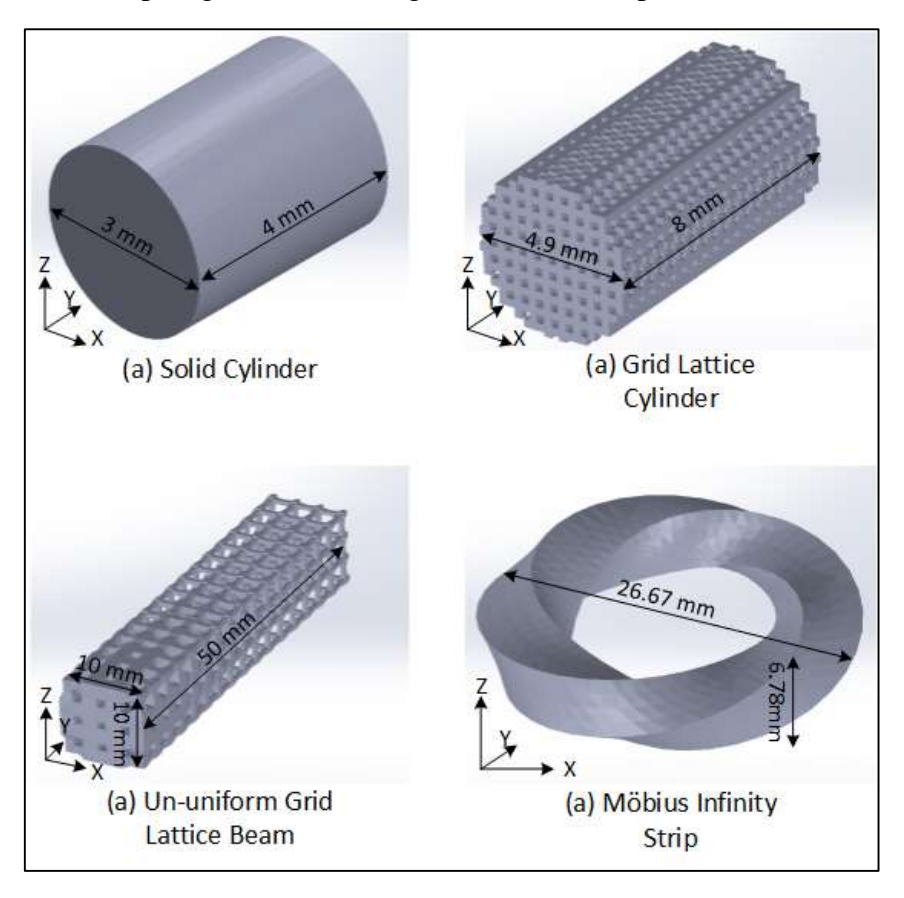


Fig. 37: Geometries for Printing Test

The variables of the printing process are the default setting of the BJ printer (suggested by © 2012 ExOne). They are listed as Table 2 and Table 3.

Table 2: Process Variables for Validation

Process Variable	Value
Layer Thickness (μm)	100
Drying Time (s)	30
Printing Saturation (%)	75
Powder Recycle Ratio (%) <sup>1</sup>	65
Cleaning Frequency	0.5

Table 3: Spread Speed

Layer	1-10	11-15	16-20	21-25	26-35	>35
Spread Speed(mm/s)	1	3	5	5	5	5
Rapid Traversing Speed (mm/s)	40	30	30	30	30	30

Fig. 38 shows the results of the simulated power curve for these part geometry and the results are compared with the experimental records.

<sup>&</sup>lt;sup>1</sup> The powder recycle ratio is derived by statistical calculation of former experiments. It is highly depends on the powder recycling process and the operators. In this research, the value is 65%.

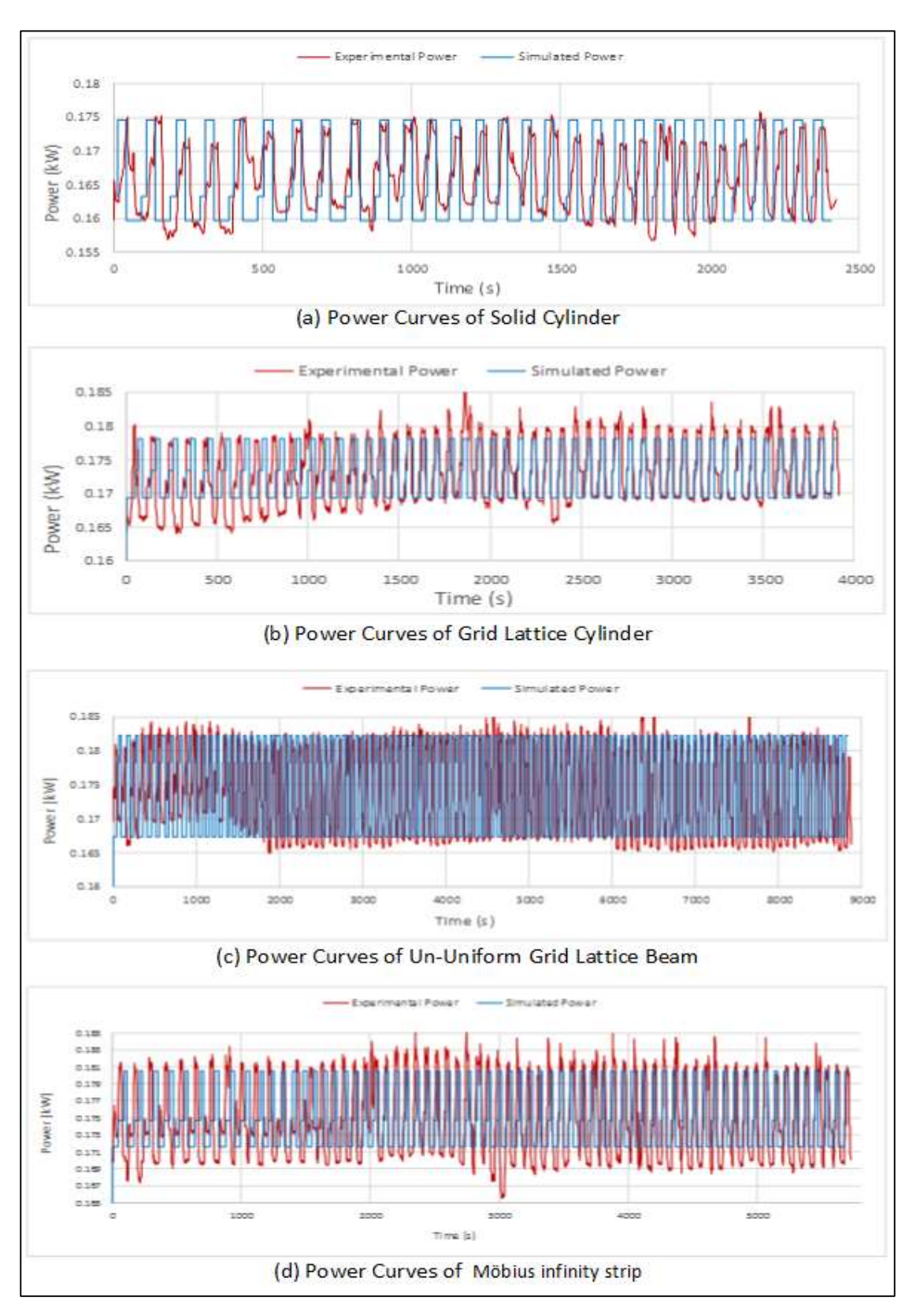


Fig. 38: Power Curves of Simulation Results and Experimental Records
The result of energy and material consumption are shown as Table 4:

Table 4: Comparison of Simulation Results and Experimental Records for Test

Part Geometries

Part				Accuracy
Geometry	Items	Simulated	Experimental	(%)
	Build-Time (s)	2408.00	2424.00	99.34
	Energy Consumption (kJ)	398.95	408.61	97.64
Solid Cylinder	Powder Consumption (kJ)	119.36	132.00	90.43
	Binder Consumption (ml)	103.80	107.00	97.01
	Cleaner Consumption (ml)	93.60	96.00	97.5
	Build-Time (s)	3906.75	3918.00	99.71
Cuid Lattice	Energy Consumption (kJ)	667.30	677.67	98.47
Grid Lattice Cylinder	Powder Consumption (kJ)	124.76	131.00	95.24
	Binder Consumption (ml)	175.40	186.00	94.30
	Cleaner Consumption (ml)	152.88	156.00	98.00
	Build-Time (s)	8840.78	8880.00	99.56
Un-Uniform	Energy Consumption (kJ)	1502.87	1540.82	97.54
Grid Lattice	Powder Consumption (kJ)	122.86	143.00	85.92
Beam	Binder Consumption (ml)	386.93	411.00	94.14
	Cleaner Consumption (ml)	336.96	341.00	98.82
	Build-Time (s)	5708.77	5722.00	99.77
3.6.4.1	Energy Consumption (kJ)	987.38	1000.08	98.73
M öbius	Powder Consumption (kJ)	123.99	139	89.20
Infinity Strip	Binder Consumption (ml)	240.33	235.00	102.27
	Cleaner Consumption (ml)	209.04	208.00	100.50

According to the comparisons shown in Fig. 38 and Table 4, while using the BJ model to simulate the energy and material consumption for the test part geometries, the largest error is (100 - 85.92)% = 14.08% which happened on the powder consumption simulation of un-uniform grid lattice beam. For the rest, most of the simulation accuracies are higher than 90%. As a conclusion, the BJ model and the simulation method can work with different part geometry properly.

### **5.1.3 Simulation of Different Process Variable**

To test if the BJ model can properly simulate the BJ process with different process variables, three compression testing cylinders are printed with 8 sets of process variables shown as Table 5.

Table 5: Process Variables for Compression Testing Cylinders

Set No.	1	2	3	4	5	6	7	8
Layer Thickness (µm)	200	200	200	150	100	50	50	50
Drying Time (s)	30	60	45	15	30	30	85	60
Binder Saturation (%)	60	90	105	105	105	75	90	105
Percentage of Drying Power <sup>2</sup> (%)	100	70	55	70	85	70	45	100
Powder Recycle Ratio (%)	65	65	65	65	65	65	65	65
Cleaning Frequency	0.5	0.5	0.5	0.5	0.5	0.5	0.5	0.5

The geometry of the testing compression test cylinders is shown as Fig. 39:

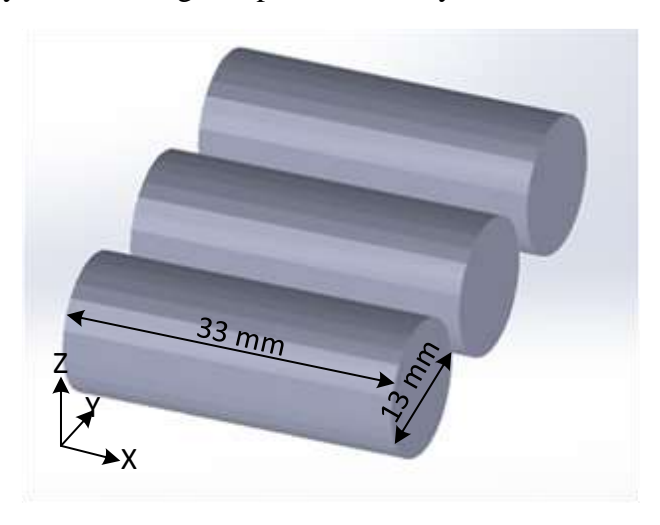


Fig. 39: Geometry of Compression Test Cylinders

For each set of variables, the build-time, energy usage and material consumption of the printing process is recorded. These records are compared with the simulation results. The comparison is shown as Table 6.

Table 6: Comparison between Experimental Records and Simulation Results

1	2	3	4
8512	10512	11260	11374
8174	10290	10747	10827
96.03	97.89	95.45	95.20
1790.65	1860.6	1843	2384
1718.45	1781.43	1765.16	2308.32
95.96	95.73	95.77	96.82
180	158	196	141
157.6	157.6	157.6	157.6
87.22	99.73	80.40	111.72
245	256	282	314
	8512 8174 <b>96.03</b> 1790.65 1718.45 <b>95.96</b> 180 157.6 <b>87.22</b>	8512 10512 8174 10290 <b>96.03 97.89</b> 1790.65 1860.6 1718.45 1781.43 <b>95.96 95.73</b> 180 158 157.6 157.6 <b>87.22 99.73</b>	8512     10512     11260       8174     10290     10747       96.03     97.89     95.45       1790.65     1860.6     1843       1718.45     1781.43     1765.16       95.96     95.73     95.77       180     158     196       157.6     157.6     157.6       87.22     99.73     80.40

<sup>&</sup>lt;sup>2</sup> If the power curve of test sample printing is provide, the drying power is calculated by the power analyzing. Otherwise, the drying power is determined by the percentage of drying power.

240	244	246	322
97.96	95.31	87.23	102.55
204	228	217	264
203	203	203	268
99.51	89.04	93.55	101.52
5	6	7	8
13373	18120	25333	19575
12501	16998	23203	17896
96.68	96.86	95.70	95.61
2554	3031	4822	3754
2488	2925	4661	3606
97.44	96.53	96.66	96.06
178	140	156	168
157.6	157.6	157.6	157.6
88.54	112.57	101.03	93.81
492	750	793	784
479	725	727	730
97.36	96.67	91.68	93.11
393	666	697	717
405	624	624	624
103.05	93.69	89.53	87.03
	97.96 204 203 99.51 5 13373 12501 96.68 2554 2488 97.44 178 157.6 88.54 492 479 97.36 393 405	97.96         95.31           204         228           203         203           99.51         89.04           5         6           13373         18120           12501         16998           96.68         96.86           2554         3031           2488         2925           97.44         96.53           178         140           157.6         157.6           88.54         112.57           492         750           479         725           97.36         96.67           393         666           405         624	97.96         95.31         87.23           204         228         217           203         203         203           99.51         89.04         93.55           5         6         7           13373         18120         25333           12501         16998         23203           96.68         96.86         95.70           2554         3031         4822           2488         2925         4661           97.44         96.53         96.66           178         140         156           157.6         157.6         157.6           88.54         112.57         101.03           492         750         793           479         725         727           97.36         96.67         91.68           393         666         697           405         624         624

According to Table 6, following conclusions are derived:

- 1. With an error tolerance of 20 %, the BJ model can simulate the BJ printing process while using different process variable: The accuracy of build-time simulation varies from 95.2 % to 97.89 %, the accuracy of energy consumption simulation varies from 95.73 % to 98.86 %, the accuracy of powder consumption simulation varies from 80.40 % to 112.57 %, the accuracy of binder consumption simulation varies from 87.23 % to 102.55% and the accuracy of cleaner consumption simulation varies 87.03 % to 103.05 %.
- 2. The results of build-time and energy consumption simulation are more accurate than the results of material consumption simulation. A possible explanation for this might be: While creating the model, the operation time and power information used for simulation is sampled by a power meter at the frequency of 1 sample per seconds. Then it is processed by the energy analyzing method (discussed in section 4.5). However, the material consumption is only measured

before and after printing which is not accurate enough. Therefore, the material consumption errors of basic operations are reflected in the final simulation results.

Combine the conclusions of section 5.1.1 and section 5.1.2, the BJ model and the simulation method in research can work with different part geometry and process variables properly. Also, the simulation result can effectively reflect the build-time, energy and material consumption of BJ printing process. Thus, the simulation method and the BJ model based on this method are valid.

#### **5.2 Simulation of test cases**

To study the characteristic of the BJ printing process, three sets of simulations are performed to reveal the energy and material consumption features of BJ technology:

- 1. A compressor wheel is simulated with different layer thickness find out the effects of layer thickness on the energy and material consumption.
- 2. Lattice structure parts with same external geometry but different internal lattice structures are simulated to find the influences of internal lattice structure.
- 3. Solid parts with different geometries are simulated with different print orientation to find out the sensitivity of print orientation for different geometry. The simulations and analyses are illustrated as following.

## 5.2.1 Effects of Layer Thickness

As shown in Fig. 40 (courtesy of Andreas), the energy and material consumed by the printing process of a compressor wheel are simulated. For the simulation, the geometry and the printing orientation are fixed.

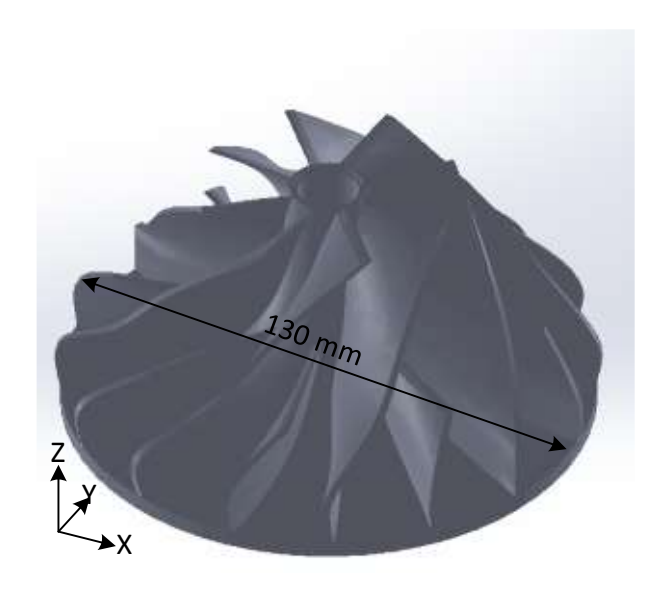


Fig. 40: Geometry of Compressor Wheel

For these simulations, the only changing process variable is the layer thickness, the rest of the process variables remains the same for different sets. The values of the process variables are listed in Table 7, the spreading speeds are the same as Table 3:

Table 7: Process Variables for Compressor Wheel

Set No.	1	2	3	4	5
Layer Thickness (µm)	100	150	200	250	300
Drying Time (s)	40	40	40	40	40
Binder Saturation (%)	70	70	70	70	70
Percentage of Drying Power (%)	75	75	75	75	75
Powder Recycle Ratio (%)	65	65	65	65	65
Cleaning Frequency	0.5	0.5	0.5	0.5	0.5

The upper limit of the layer thickness is chosen as 300  $\mu m$ . The reason for choosing such a value is when the layer is thicker than 300  $\mu m$ , the binder can hardly diffuse through the whole thickness of layer (suggested by suggested by © 2012 ExOne). Therefore, layer thicker than 300 300  $\mu m$  are not using in real manufacturing. To make the manufacturing of the compressor wheel feasible, the build-volume of printer is changed into 140 x 140 x 70 mm. The simulation results are shown in Table 8.

Table 8: Energy and Material Consumption of Different Layer Thicknesses

Set No.	1	2	3	4	5
Number of Slices	600.00	450.00	300.00	240.00	200.00

<b>Build-Time</b> (s)	55599.16	37120.61	27753.72	22084.81	18556.98
<b>Energy Consumption (kJ)</b>	9199.28	6141.90	4592.05	3654.11	3070.41
Powder Consumption (g)	510.92	510.32	509.26	508.60	508.17
<b>Binder Consumption (ml)</b>	2192.77	1480.47	1118.86	900.46	764.40
Cleaner Consumption (ml)	1868.88	1248.00	932.88	742.56	624.00

The results of the simulation for different layer thicknesses show that:

- 4. The build-time, energy consumption, binder consumption and cleaner consumption are significantly affected by the layer thickness: on average, these values for 0.3 mm layer thickness are 66.3 % less than the values for 0.1mm. A thinner layer thickness will increase the number of slices being fabricated. As a result, the build-time of the whole part manufacturing will increase as well as the total process energy consumption. With the increasing of slices, the times of flushing and cleaning operations of printhead also increase which result in a greater usage of binder and cleaner.
- 5. Powder consumption do not seem affected by the layer thickness as it is determined by the volume of the part.

#### **5.2.2 Effects of Internal Lattice Structure**

Cuboids with different internal lattice structures are simulated to study the influences of internal lattice structure on the BJ printing process. The external dimensions of the cuboids are uniform:  $40 \, \text{mm} \times 40 \, \text{mm} \times 30 \, \text{mm}$ . The internal lattice structure form is grid. The lattice structures are generated by WITHIN ENHANCE (© MMXI WithinLab). As shown in Fig. 41, the strut thicknesses of lattice structure vary from 0.2 mm to 0.7 mm in increments of 0.1 mm.

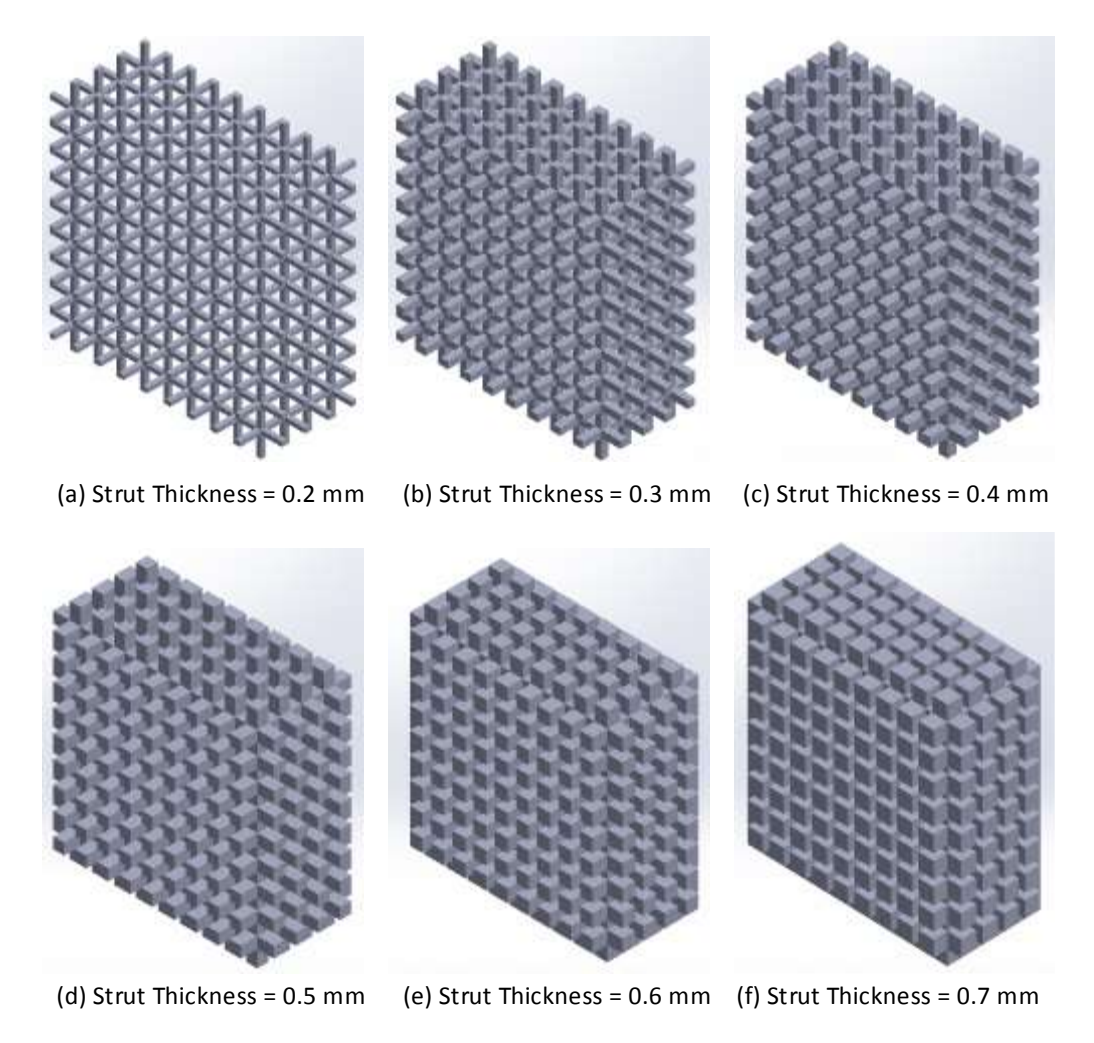


Fig. 41: Internal Lattice Structure of Different Strut Thickness

The processes variables are the same as Table 2 and Table 3. Results of simulation are shown as

Table 9: Energy and Material Consumption of Different strut Thickness

Lattice Thickness	0.2	0.3	0.4	0.5	0.6	0.7
<b>Build-Time</b> (s)	34778.15	34801.42	34822.64	34841.56	34858.31	34874.60
Energy Consumption (kJ)	5782.07	5785.83	5789.27	5792.33	5795.04	5797.68
Powder Consumption (g)	211.12	353.22	470.85	650.95	834.61	974.36
Binder Consumption (ml)	1800.94	1818.72	1833.43	1855.97	1878.94	1896.43

Cleaner						
Consumption	1560.00	1560.00	1560.00	1560.00	1560.00	1560.00
(ml)						

Analyzing the data in Table 8, following statements can be concluded:

- 6. The build-time, energy consumption and cleaner usage of BJ printing process are determined by the external geometry of the part. The change of internal structure hardly affects them.
- 7. The powder and binder consumption of the printing process is relevant to the internal structure of part. These two consumption increase with the increasing the part geometry.

### **5.2.3** Sensitivity of Print Orientation

Generally speaking, for AM processes, print orientation will affect the process build-time, energy usage and material consumption. However, let us consider a special situation: to fabricate a solid ball by AM technologies. Under this situation, as ball is **spherical symmetry**, the printing process should be the same on any print orientation. In other words, the print orientation does not have influence on the energy and material consumption of the fabrication process of the ball. Therefore, different geometries have different sensitivity to print orientation. To find out the sensitivity of print orientation for different geometry, simulations of different part are performed in this section.

Before conducting the simulation and analyzing the result, the **Longest print** height and Shortest print height Ratio (LSR) is introduced here. The LSR is a characteristic of part geometry. As shown in Fig. 42, the Longest print Height (LH) equals to the longest distance between two points on the part while the Shortest print Height (SH) is the shortest edge of the minimal bonding box of the part.

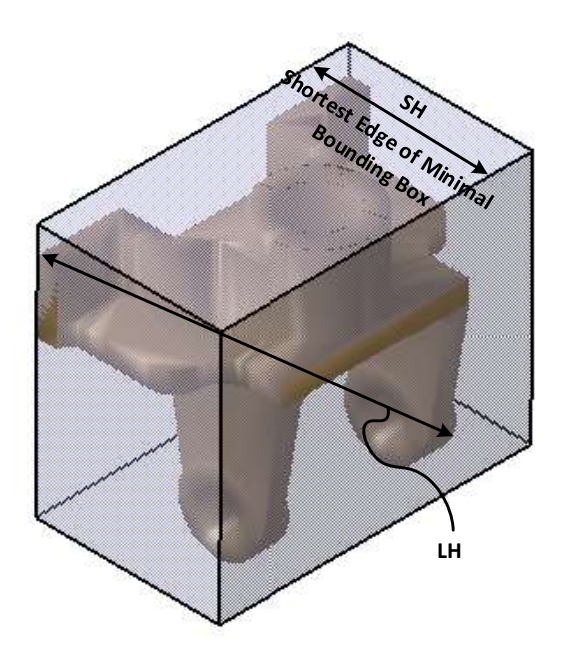


Fig. 42: LH and SH on a part

Then LSR is define as:

$$LSR = \frac{LH}{SH}$$
.

Two parts shown in Fig. 43 are simulated with different print orientations vary from 0° to 180° with increments of 30°. Fig. 43 (a) shows a mechanical support (courtersy of Sudhir Gill) with a LSR of 2.38. The print orientation refers to the angle  $\gamma$  between the build orientation vector  $\vec{Z}$  and the normal vector of the planar surface  $\vec{n}_p$ . Fig. 43 (b) shows a spring with a LSR of 5.07. The print orientation refers to the angle  $\gamma$  between the build orientation vector  $\vec{Z}$  and the axis of the spring  $\vec{sa}$ .

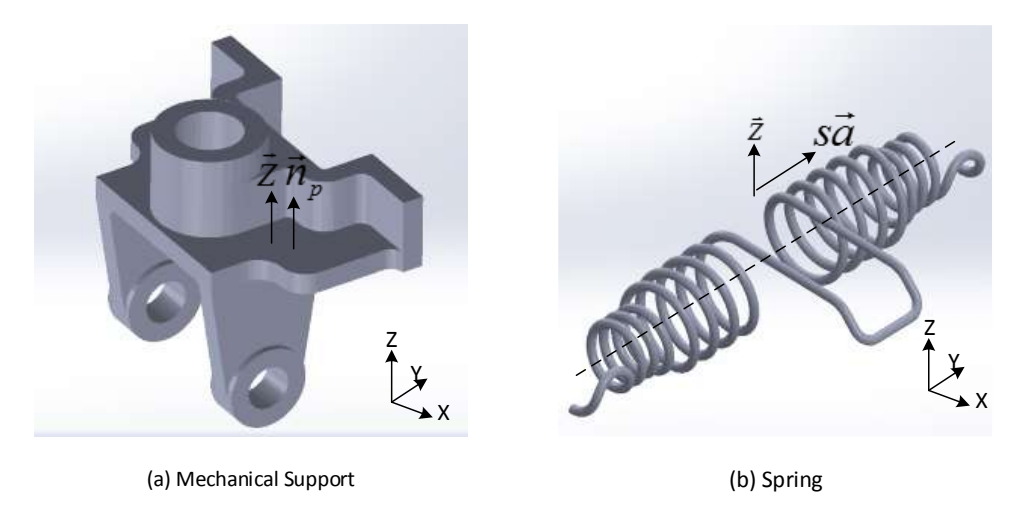


Fig. 43: Geometry of Mechanical Support and Spring

The processes variables for simulations are shown Table 10. The spread speeds are set as Table 3.

Table 10: Process Variables for Validation

Process Variable	Value
Layer Thickness (µm)	300
Drying Time (s)	30
Printing Saturation (%)	75
Powder Recycle Ratio (%)	65
Cleaning Frequency	0.5

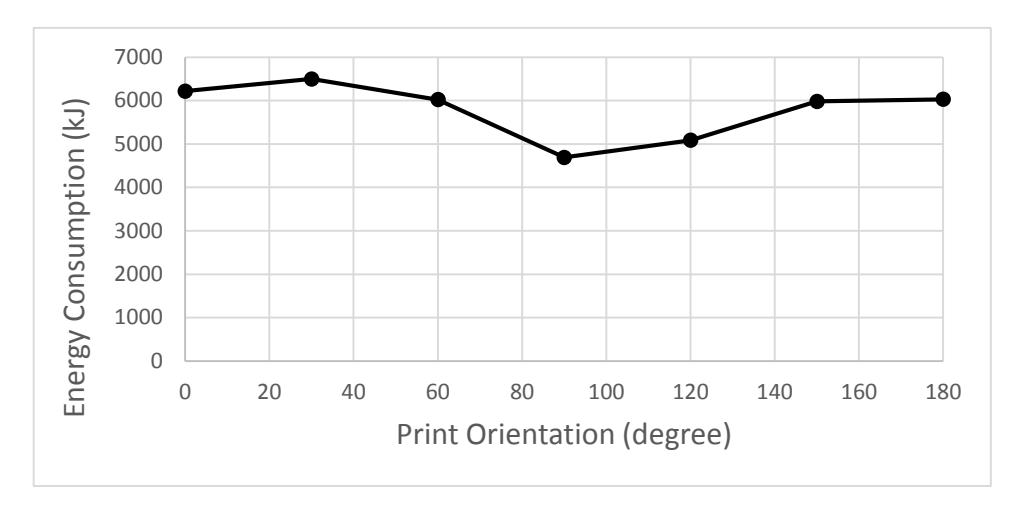
The results of simulation are listed as Table 11:

Table 11: Energy and Material Consumption for Different Print Orientation

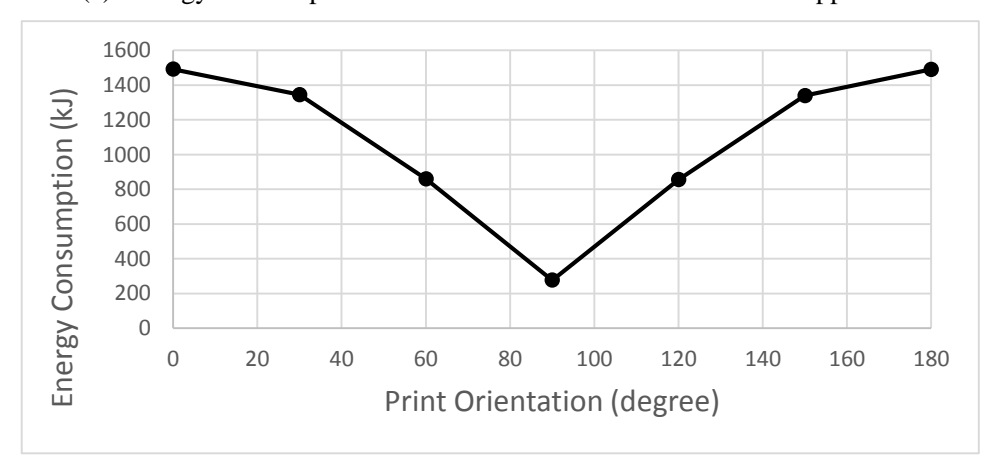
	D 1 4							
	Print Orientati	0	30	60	90	120	150	180
	on (°)							
	Build-	37597.77	39323.48	36450.21	28389.51	30751.87	36162.69	36479.53
	Time (s)	37371.77	37323.10	30 130.21	20307.31	30731.07	30102.09	30477.33
	Energy							
	Consump	6215.84	6495.57	6020.82	4690.46	5083.82	5980.06	6029.63
Mechanica	tion (kJ)							
l Support	Powder							
TSupport	Consump	799.60	799.78	799.70	800.02	800.22	800.17	800.58
	tion (g)							
	Binder							
	Consump	1552.45	1609.74	1455.83	1123.03	1237.58	1520.31	1538.26
	tion (ml)							
	Cleaner							
	Consump	1279.20	1329.12	1194.96	904.80	1004.64	1251.12	1266.72
	tion (ml)							
	Print							
	Orientati	0	30	60	90	120	150	180.00
	on							
Spring	Build-	8964.03	8087.00	5170.99	1661.44	5143.32	8053.99	8959.91
	Time (s)	0704.03	0007.00	5170.73	1001.44	5175.52	0033.77	0,3,7.71
	Energy							
	Consump	1490.88	1344.82	859.83	276.25	855.21	1339.30	1490.20
	tion (kJ)							

Powder							_
Consump	120.02	120.02	120.02	120.02	120.01	120.01	120.02
tion (g)							
Binder							
Consump	468.89	415.20	261.31	82.36	261.31	415.20	468.89
tion (ml)							
Cleaner							
Consump	408.72	361.92	227.76	71.76	227.76	361.92	408.72
tion (ml)							

Fig. 44 shows a comparison on the energy consumption for different print orientation between the mechanical support and spring.



(a) Energy Consumption vs. Print Orientation for Mechanical Support



(b) Energy Consumption vs. Print Orientation for Spring Support

Fig. 44: Energy Consumption of Different Print Orientation

The ratio between maximum energy consumption and the minimum energy consumption of the mechanical support is 1.38 while it is 5.40 for the spring. Thus, the energy consumption of spring is more sensitive to the print orientation. Compare the

material consumption, the same result can be concluded. This result indicates the sensitivity of print orientation is relevant to the value of LSR. Part of lager LSR value, its' energy and material consumption is more sensitive to the print orientation.

To give a quantified relationship of the print orientation sensitivity and LSR, series of cuboids with different LSR are simulated. As shown in Fig. 45, for the cuboid, the LH is the length of space diagonal and the SH is the length of the shortest edge.

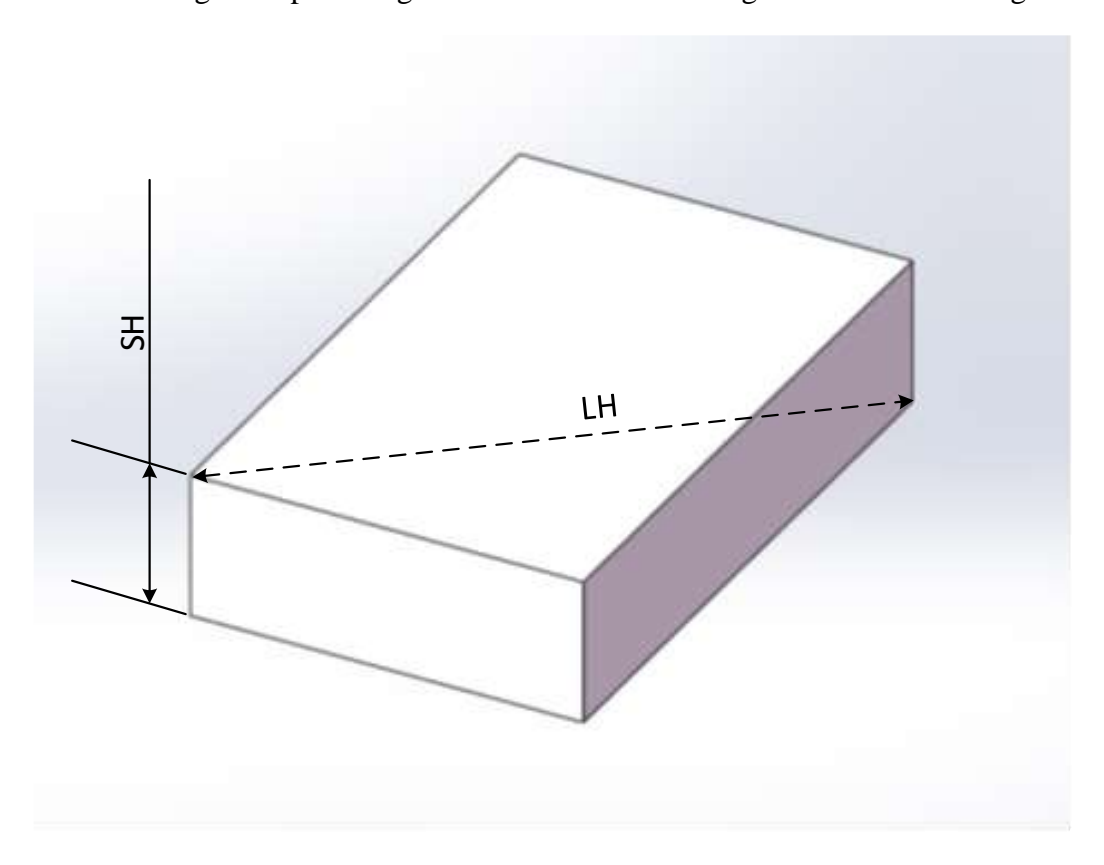


Fig. 45: LH and SH of Cuboid

The LSR varies from 1.8 to 5.0 with an increment of 0.1. The Ratio between Maximum energy consumption and the Minimum energy consumption (RMM) are used to represent the sensitivity of print orientation. In this research, define while the RMM is greater than 2, the part is sensitive to the print orientation. The processes variables for simulations are the same as Table 2 and Table 3.

Fig. 46 shows the result of simulation of cuboid with different RMM values.

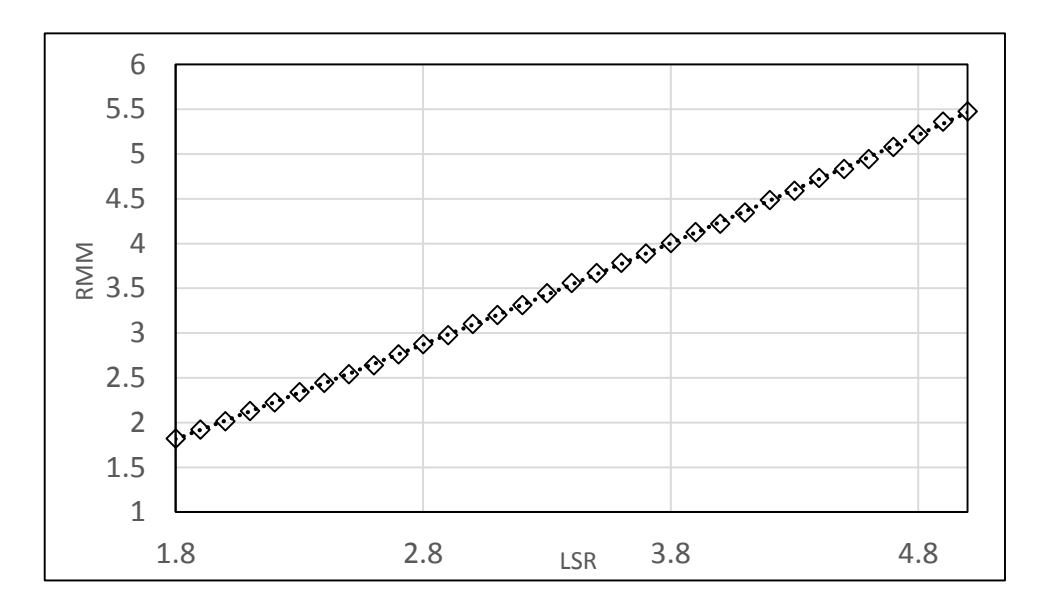


Fig. 46: LSR vs. RMM for Cuboid

Fig. 46 reveals that the RMM increases with the LSR. A 2-degree polynomial regression with bi-square objective function and 95% confident bound is performed to process the LSR vs. RMM curve (linear regression are also performed, however, the R-square value of linear regression is 97.92% while it is 99.35% for the 2 degree polynomial regression. Thus, the data is closer to the 2 degree polynomial equation). Therefore, in the interval of 1.8 and 5, the LSR and RMM have relationship as:

$$RMM = 0.03569LSR^2 + 0.8921LSR + 0.1059$$

Therefore, while RMM=2, the value of LSR is solved as 1.968 (solution less than 0 is discarded). This conclusion suggests that while the LSR is greater than 1.968, the print orientation will significantly influence the energy and material consumption of the BJ printing process. As a result, the user of the 3D printer should consider to find an optimal print orientation to achieve better energy and material performance of the printing.

# Chapter 6: Conclusion and future scope of research

Up to this point, a simulation method was developed to calculate the build-time, energy usage and material consumption of AM technologies. Afterward, this method was adapted on the BJ technology and an energy and material consumption model of BJ is achieved. Then the validation of the BJ model was performed. After the validation, a series of case studies were conducted and the characteristics of energy and material consumption and build-time of BJ technology were analyzed base on the case studies. As the last chapter of the dissertation, this chapter will summarise the main finding of the above works. Furthermore, for the research scope which was defined in section 1.2, several limitations are caused due the research scope. These limitations will be discussed in this chapter. It will then conclude with suggestions of possible ways to improve the quality of modelling and the future works.

#### **6.1 Conclusions**

The first goal of this study is to develop a simulation method to calculate the energy and material consumption of AM technologies. More specifically, if a part is designed by a CAD system and output to be fabricated by an AM technology, by input the part geometry, print orientation and process variables into the simulation method, the build-time, energy usage, material consumption of the part manufacturing can be estimated before the real printing. As discussed in Chapter 1, the AM technologies create parts by generating contiguous slices layer by layer. Based on this characteristic, the simulation method focusses on the layer fabrication level of AM processes. Then results of each layer's simulation are summed together to achieve the result of the whole manufacturing process of AM. This method allows AM designers and practitioners to predict the build-time, energy usage and material consumption of part which produced by AM and correlate this consumables to the part geometry, process variables. Hence, the simulation method provides a tool for AM designer to optimize the part geometry to achieve a better energy or material performance. Also, it can assist the AM user to pick process variables to meet the requirement of build-time, energy usage or material consumption constraints of the manufacturing.

A slicing method was realized in this research to process the part geometry which is saved as STL file. The slicing method was presented in the section 3.4. With this slicing method, a part is sliced into a series of layer contours. These contours contain the geometry information which is needed for the printing process. Then, the geometry information are provided to the simulation method to conduct the virtual AM process which was discussed in section 3.3. To perform the slicing process, the following input variables are needed: part geometry, print orientation and layer thickness. When these three variables are given, a program will intersect the 3D part geometry by a group of planes and save the intersections for the simulation. These planes are perpendicular to print orientation and the distance between two adjacent planes is the values of layer thickness. Through the slicing method, the geometry of part is processed to generate the shape of slices, and the shape of slices is used in the simulation. Thus, the geometry information is imported by the slicing method. In this research, the slicing method is the fundamental to develop a simulation method which can consider part geometry as a variable.

In Chapter 4, the simulation method was adapted to the BJ process. As a result, an energy and material consumption model of BJ process was created. According to the simulation method, to build the BJ model, three kinds of information are required: basic operations of BJ, the power and material consumption of basic operations and the operation time of the basic operations. To achieve basic operations, IDEF0 method was employed in this research to decompose the printing process of BJ. By analyzing, in BJ, each slice is fabricated by three operations: drying printed layer, spreading new layer and printing new layer. As the part is built by repeating the fabrication of slices, the whole printing process is represented by an operation list which made up of the above three basic operations. The motion and material consumption characteristics of these three basic operations were studied to derive the relations between the operation time, material consumption and process variables. In addition, a power analyzing method was developed to process power data of the BJ printing process and generate the power information of each basic operations. This BJ model allows the user to predict the build-time energy and material consumption of BJ process. Also, the validation of the BJ

process was performed to check the correctness and the quality of the model. If the BJ model is accurate enough, then it is reasonable to say the simulation method is effective.

Finally, energy and material consumption of test cases were calculated with the BJ model to reveal the energy and materials consumption characteristics of BJ technology. In Section 5.2.1 printing processes of a compressor with different layer thickness are simulated. The result showed the layer thickness has obvious effects on the build-time, energy usage and cleaner usage. In section 5.2.2, part with same external geometry but different internal lattice structures were input to the BJ model. The results revealed the build-time, energy usage and cleaner consumption are determined by the external geometry while the powder usage and binder consumption are affected by the internal structures.

Additionally, print orientation sensitivity of different part geometry was studied. The manufacturing processes of a mechanical support structure and a spring were simulated. The print orientations of the three parts varied from 0° to 180°. The simulation result showed, for the energy and material consumption, different geometries have different sensitivities of print orientation. According to the conclusion of section 5.2.3, while the RMM is greater than 1.968, the energy and material consumption of part manufacturing is significantly affected by the print orientation.

## **6.2 Future Scope of Research**

This research is only one of the first several steps to transfer AM from an advanced lab based prototyping method to a mature industrial manufacturing. The simulation method developed in this research still has a number of limitations. These limitations and the corresponding possible improvements are discussed as following.

As discussed in section 1.2, the scope of the research is the unit-process of AM. Thus, the simulation method developed in this research only focuses on the individual AM machine and the 3D printing process. Although AM is a highly centralized: most of the manufacturing processes are finished by the AM machine, there are still some auxiliary processes for AM. For instance, the BJ technology needs curing and sintering processes to produce the final functional part. Also, finishing or milling process is often

conducted to improve the surface quality of AM part. Therefore, to achieve a more comprehensive model for AM, the simulation method developed by this research should cooperate with other energy and material simulation methods of the auxiliary processes, such as finishing, milling, sintering. As a result, a line/cell/multi-machine system level simulation method can be developed.

Future work can also add the emission calculation module to the simulation method. The current simulation method didn't consider the waste and emissions of AM in the calculation. However, every AM will generate waste and emissions. For instance, waste heat and inert protective gas emission are very common exhausts in AM technologies (such as SLS, SLM, FMD and BJ) which sinter/melt powders and form parts. By adding the waste and emissions calculation module, the simulation method can provide a more complete LCI data for AM technologies.

### Reference

- [1] Petrovic, V., 2011, Additive layered manufacturing: sectors of industrial application shown through case studies.
- [2] Bourell, D. L., Leu, M. C., and Rosen, D. W., 2009, Roadmap for Additive Manufacturing-Identifying the Future of Freeform Processing The University of Texas at Austin Laboratory for Freeform Fabrication Advanced Manufacturing Center.
- [3] Schipper, M., 2006, "Energy-Related Carbon Dioxide Emissions in U.S. Manufacturing," No. DOE/EIA-0573(2005).
- [4] 2010, Energy Technology Perspective 2010 -Scenario & strategies to 2050, International Energy Agency (IEA).
- [5] Morrow, W. R., Qi, H., Kim, I., Mazumder, J., and Skerlos, S. J., 2007, "Environmental aspects of laser-based and conventional tool and die manufacturing," Journal of Cleaner Production, 15(10), pp. 932-943.
- [6] Sreenivasan, R., Goel, A., and Bourell, D. L., 2010, "Sustainability issues in laser-based additive manufacturing," Physics Procedia, 5, Part A(0), pp. 81-90.
- [7] Camposeco-Negrete, C., 2013, "Optimization of cutting parameters for minimizing energy consumption in turning of AISI 6061 T6 using Taguchi methodology and ANOVA," Journal of Cleaner Production, 53(0), pp. 195-203.
- [8] Mori, M., Fujishima, M., Inamasu, Y., and Oda, Y., 2011, "A study on energy efficiency improvement for machine tools," CIRP Annals Manufacturing Technology, 60(1), pp. 145-148.
- [9] Rajemi, M. F., Mativenga, P. T., and Aramcharoen, A., 2010, "Sustainable machining: selection of optimum turning conditions based on minimum energy considerations," Journal of Cleaner Production, 18(10–11), pp. 1059-1065.
- [10] Li, L., Yan, J., and Xing, Z., 2013, "Energy requirements evaluation of milling machines based on thermal equilibrium and empirical modelling," Journal of Cleaner Production, 52(0), pp. 113-121.
- [11] Duflou, J. R., Sutherland, J. W., Dornfeld, D., Herrmann, C., Jeswiet, J., Kara, S., Hauschild, M., and Kellens, K., 2012, "Towards energy and resource efficient manufacturing: A processes and systems approach," CIRP Annals Manufacturing Technology, 61(2), pp. 587-609.
- [12] European\_Commission, and Joint\_Research\_Centre, 2010, International Reference Life Cycle Data System (ILCD) Handbook General guide for Life Cycle Assessment Detailed guidance.
- [13] Ashby, M. F., 2012, Materials and the Environment, 2nd Edition, Butterworth Heinemann.

- [14] 1998, "ISO 14040 Environmental managementd Life cycle assessmentd Principles and framework: International Organisation for Standardisation," Geneva, Switzerland.
- [15] Vigon, B., Tolle, D., Cornaby, B., Latham, H., Harrison, C., Boguski, T., and et al, 1993 EPA/600/R-92/245, "Life Cycle Assessment: Inventory Guidelines and Principles," U. E. P. A. (EPA), ed.
- [16] Fava, J., Denison, R., Jones, B., Curran, M., Vigon, B., Selke, S., and et al, 1991, "A Technical Framework for Life-Cycle Assessment," U. SETAC, ed. Washington.
- [17] Consoli, F., Allen, D., Boustead, I., Fava, J., Franklin, W., Jensen, A., and et al, 1993, "Guidelines for Life-Cycle Assessment: A 'Code of Practice'," SETAC, ed.
- [18] Suh, S., and Huppes, G., 2005, "Methods for Life Cycle Inventory of a product," Journal of Cleaner Production, 13(7), pp. 687-697.
- [19] Heijungs, R., 1994, "A generic method for the identification of options for cleaner products," Ecological Economics, 10(1).
- [20] 2001, SYSTEMS ENGINEERING FUNDAMENTALS, DEFENSE ACQUISITION UNIVERSITY PRESS.
- [21] Ross, D. T., 1977, "Structured Analysis (SA): A Language for Communicating Ideas," Software Engineering, IEEE Transactions on, SE-3(1), pp. 16-34.
- [22] Kim, S.-H., and Jang, K.-J., 2002, "Designing performance analysis and IDEF0 for enterprise modelling in BPR," International Journal of Production Economics, 76(2), pp. 121-133.
- [23] Busby, J. S., and Williams, G. M., 1993, "The value and limitations of using process models to describe the manufacturing organization," International Journal of Production Research, 31(9), pp. 2179-2194.
- [24] Bravoco, R. R., and Yadav, S. B., 1985, "A methodology to model the functional structure of an organization," Computers in Industry, 6(5), pp. 345-361.
- [25] Sarkis, J., and Lin, L., 1994, "An IDEF0 functional planning model for the strategic implementation of CIM systems," International Journal of Computer Integrated Manufacturing, Vol. 7 No.2, pp. pp. 100-115.
- [26] Kusiak, A., Nick Larson, T., and Wang, J., 1994, "Reengineering of design and manufacturing processes," Computers & Industrial Engineering, 26(3), pp. 521-536.
- [27] Kim, C., Kim, K., and Choi, I., 1993, "An object-oriented information modeling methodology for manufacturing information systems," Computers & Industrial Engineering, 24(3), pp. 337-353.
- [28] Lee, K. H., and Woo, H., 2000, "Direct integration of reverse engineering and rapid prototyping," Computers & Industrial Engineering, 38(1), pp. 21-38.
- [29] Paul, B., 1999, "STL format," http://paulbourke.net/dataformats/stl/.

- [30] Figueiredo, M., Ribeiro, B., and de Almeida, A., 2014, "Electrical Signal Source Separation Via Nonnegative Tensor Factorization Using On Site Measurements in a Smart Home," Instrumentation and Measurement, IEEE Transactions on, 63(2), pp. 364-373.
- [31] Schmidt, M. N., and Olsson, R. K., 2006 September, "Single-channel speech separation using sparse non-negative matrix factorization," International Conference on Spoken Language Processing.
- [32] Kolter, J. Z., Batra, S., and Ng, A. Y., "Energy Disaggregation via Discriminative Sparse Coding," Proc. Advances in Neural Information Processing Systems 23, J. Lafferty, C. Williams, J. Shawe-taylor, R. s. Zemel, and A. Culotta, eds., pp. 1153-1161.
- [33] Hart, G. W., 1989, "Residential energy monitoring and computerized surveillance via utility power flows," Technology and Society Magazine, IEEE, 8(2), pp. 12-16.
- [34] Hart, G. W., 1992, "Nonintrusive appliance load monitoring," Proceedings of the IEEE, 80 (12) (Dec. 1992), pp. 1870-1892.
- [35] Canny, J., 1986, "A Computational Approach to Edge Detection," Pattern Analysis and Machine Intelligence, IEEE Transactions on, PAMI-8(6), pp. 679-698.
- [36] Marceau, M. L., and Zmeureanu, R., 2000, "Nonintrusive load disaggregation computer program to estimate the energy consumption of major end uses in residential buildings," Energy Conversion and Management, 41(13), pp. 1389-1403.
- [37] Blinchikoff, H. J., and Zverev, A. I., 2001, Filtering in the Time and Frequency Domains, SciTech Publishing; New edition edition.